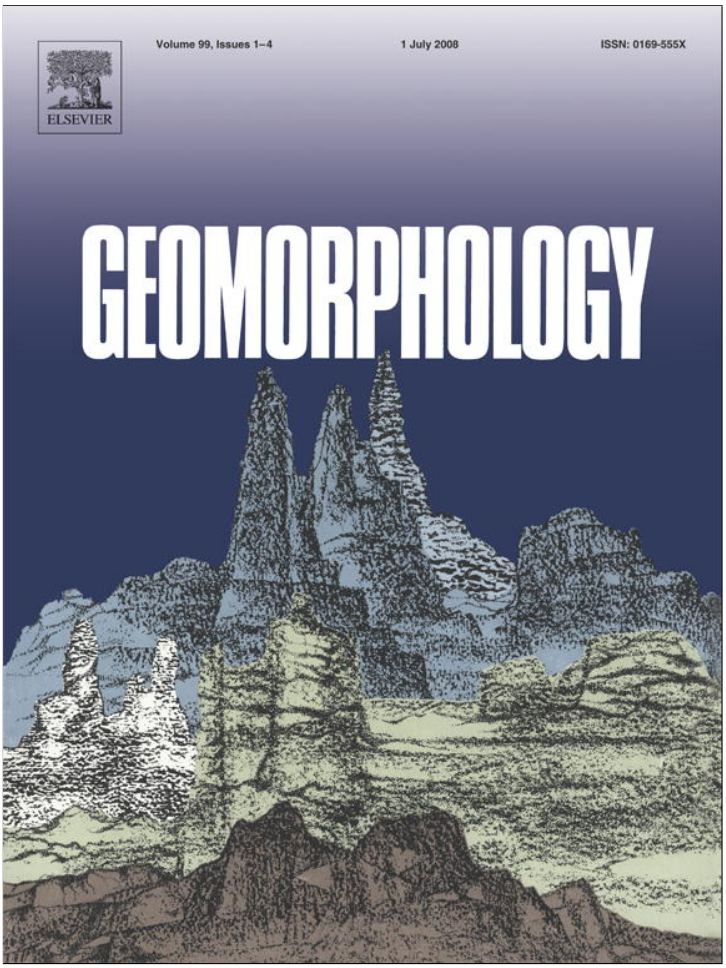

Available online at www.sciencedirect.com
ScienceDirect
Geomorphology 99 (2008) 39–58
GEOMORPHOLOGY
www.elsevier.com/locate/geomorph

Susceptibility and triggering scenarios at a regional scale for shallow landslides

G. Gullà, L. Antronico *, P. Iaquinta, O. Terranova

National Research Council, Research Institute for Geo-Hydrologic Protection, Via Cavour 4-6, 87036 Rende, Italy

Received 23 May 2007; received in revised form 9 October 2007; accepted 10 October 2007
Available online 23 October 2007

Abstract

The work aims at identifying susceptible areas and pluviometric triggering scenarios at a regional scale in Calabria (Italy), with reference to shallow landsliding events. The proposed methodology follows a statistical approach and uses a database linked to a GIS that has been created to support the various steps of spatial data management and manipulation. The shallow landslide predisposing factors taken into account are derived from (i) the 40-m digital terrain model of the region, an ~15,075 km^2 extension; (ii) outcropping lithology; (iii) soils; and (iv) land use. More precisely, a map of the slopes has been drawn from the digital terrain model. Two kinds of covers [prevalently coarse-grained (CG cover) or fine-grained (FG cover)] were identified, referring to the geotechnical characteristics of geomaterial covers and to the lithology map; soilscapes were drawn from soil maps; and finally, the land use map was employed without any prior processing.

Subsequently, the inventory maps of some shallow landsliding events, totaling more than 30,000 instabilities of the past and detected by field surveys and photo aerial restitution, were employed to calibrate the relative importance of these predisposing factors.

The use of single factors (first level analysis) therefore provides three different susceptibility maps. Second level analysis, however, enables better location of areas susceptible to shallow landsliding events by crossing the single susceptibility maps.

On the basis of the susceptibility map obtained by the second level analysis, five different classes of susceptibility to shallow landsliding events have been outlined over the regional territory: 8.9% of the regional territory shows very high susceptibility, 14.3% high susceptibility, 15% moderate susceptibility, 3.6% low susceptibility, and finally, about 58% very low susceptibility.

Finally, the maps of two significant shallow landsliding events of the past and their related rainfalls have been utilized to identify the relevant pluviometric triggering scenarios. By using 205 daily rainfall series, different triggering pluviometric scenarios have been identified with reference to CG and FG covers: a value of 365 mm of the total rainfall of the event and/or 170 mm/d of the rainfall maximum intensity and a value of 325 mm of the total rainfall of the event and/or 158 mm/d of the rainfall maximum intensity are able to trigger shallow landsliding events for CG and FG covers, respectively.

The results obtained from this study can help administrative authorities to plan future development activities and mitigation measures in shallow landslide-prone areas. In addition, the proposed methodology can be useful in managing emergency situations at a regional scale for shallow landsliding events triggered by intense rainfalls; through this approach, the susceptibility and the pluviometric triggering scenario maps will be improved by means of finer calibration of the involved factors.

Keywords: Shallow landslide; Susceptibility; Rainfall; GIS; Calabria

1. Introduction

Shallow landslides are common in almost every area of the world and affect different geoenvironmental contexts in terms of climate, lithology, soil cover, slope morphology, vegetation, etc. The dangerousness of these phenomena, because of their rapid kinematic evolution and large areal diffusion, has been frequently pointed out in the literature. Rainfall is their main

* Corresponding author. Tel.: +39 984 835478; fax: +39 984 835319.
E-mail addresses: giovanni.gulla@irpi.cnr.it (G. Gullà), loredana.antronico@irpi.cnr.it (L. Antronico), pasquale.iaquinta@irpi.cnr.it (P. Iaquinta), oreste.terranova@irpi.cnr.it (O. Terranova).

0169-555X/$ - see front matter © 2007 Elsevier B.V. All rights reserved.
doi:10.1016/j.geomorph.2007.10.005

triggering cause. Frequently, a number of shallow landslides are observed during a single rainy season in the same area. Among the predisposing factors, a key role is played by the morphological characteristics of the slope, by the geotechnical characteristics of the geomaterials where shallow landslides develop, as well as by the impact of anthropic activities on a given area. As far as soils are concerned, these phenomena have been observed to specifically affect eluvial and/or colluvial deposits; degraded and/or weathered sedimentary and crystalline–metamorphic rocks; as well as glacial, fluvial and glacial, and pyroclastic deposits (Govi and Mortara, 1981; Moser and Hohensinn, 1983/84; Loye-Pilot, 1984; Ogura and Filho, 1991; Van Asch and Sukmantalya Kesumajaya, 1993; Aleotti et al., 1996; Wieczorek et al., 2001; D'Amato Avanzi et al., 2004).

The triggering mechanisms of landsliding phenomena and their evolution cause severe risk for a number of vulnerable elements (houses and buildings, roads, railway infrastructures, telecommunication systems, etc.). In order to be effective, risk mitigation measures should focus on the identification and accurate definition of areas susceptible to shallow landslides. In the literature, several methods are proposed to evaluate the landsliding susceptibility of an area, such as landslide inventories, heuristic approaches, statistical analyses, and deterministic approaches (Soeters and van Westen, 1996; Aleotti and Chowhury, 1999; Ermini et al., 2005). Surveys and observations that are subject to individual interpretation are the basis of the first two approaches; the third approach can be better employed in homogeneous zones or in areas with only a few types of slope instability processes (Ermini et al., 2005). The latter is essentially a geotechnical approach; therefore, data relevant to the geometry of involved slopes are needed, along with data related to the critical condition of pore-water pressure and to the physical and mechanical characteristics of involved geomaterials. The Artificial Neural Networks, the Fuzzy logic approach, and Logistic Regression Analyses can be encompassed within the framework of statistical approaches (Carrara and Guzzetti, 1995; Soeters and van Westen, 1996; Aleotti and Chowhury, 1999; Casagli et al., 1999; Clerici et al., 2002; Sorriso-Valvo, 2002; Pike et al., 2003; Ercanoglu and Gokceoglu, 2004; Ermini et al., 2005; Greco et al., 2007). Important contributions by Can et al. (2005), Gomez and Kavzoglu (2005), Guinau et al. (2005), and Guzzetti et al. (2006) are specifically useful for the statistical approach and, in particular, in relation to the problem of shallow landslides.

Calabria (southern Italy) is affected by superficial landsliding phenomena triggered by intense precipitation, that involves almost all outcropped lithologies. Research carried out over different areas and sites in Calabria (Antronico and Gullà, 2000; Antronico et al., 2002, 2004; Sorriso-Valvo et al., 2004) have produced results that are the basic elements of this study, i.e., susceptibility to shallow landsliding and triggering scenarios at a regional scale.

After describing the predisposing factors and the triggering causes of observed phenomena, the study focuses on knowledge necessary to develop the methodology used to identify areas susceptible to superficial landsliding on natural slopes and their potential triggering scenarios. The discussion of the results obtained provides useful information for the systematic use of the proposed methodology and its improvement.

2. Geoenvironmental features

2.1. Geological and geomorphological sketches

The geological complexity of Calabria is the result of the tectonic history of the region during its formation. Almost the entire region is made up of crystalline–metamorphic nappe units, defined as Calabrian Arc (Amodio-Morelli et al., 1976; Tortorici, 1982). The Calabrian Arc is an arcuate portion of the southern Apennine–Maghrebian orogenic belt (trending NW–SE and E–W, respectively). It is considered a fragment of a Europe-vergent Alpine range, overthrust as a unit during the Lower Miocene on the African-vergent Apennine–Maghrebian range during its formation (Amodio-Morelli et al., 1976; Bonardi et al., 1982; Tortorici, 1982). Its formation is also related to the opening of the Tyrrhenian Sea.

During the Late Pliocene–Early Quaternary times, the Calabrian Arc has been dissected by several normal fault segments, both longitudinally (from NE–SW to NNW–SSE) and transversally (from E–W to WNW–ESE) with respect to the trend of the arc (Ghisetti, 1979; Monaco and Tortorici, 2000; Tortorici et al., 2002). These structures caused the fragmentation of the Calabrian Arc into sedimentary basins (Crati basin, Catanzaro basin, Mesima–Gioia Tauro basin) where continental and marine sediments settled; fragmentation also caused the formation of structural highs (Coastal Range, Sila Massif, Capo Vaticano high, Aspromonte–Serre Massif).

Since the Middle Pleistocene, the whole Calabrian Arc was affected by a strong regional phase of extension, together with an intense regional uplifting (Tortorici et al., 1995; Monaco et al., 1996). This rapid Quaternary uplift of Calabria, combined with the eustatic absolute sea level changes, generated several orders of marine terraces evident along the coasts and in the tectonic valleys. Tectonic uplifting is still an ongoing process, witnessed by the intense seismic activity of the region (Westaway, 1993; Tortorici et al., 2002).

From a geological point of view and considering its structural highs and subsiding basins originated since the Pliocene, Calabria could be divided into two different sectors (Fig. 1).

The first sector in the north is formed by nappe units made up of granite rocks and by high- and low-grade metamorphic and ophiolitic rocks (Coastal Chain and the Sila Massif). These nappe are laid on carbonatic units belonging to the Appenine Chain; and the carbonatic units outcrop in the Pollino Massif and in the Coastal Chain. Marine and continental deposits, dating back to the Early Tortonian–Early Pliocene and to the Middle–Upper Pliocene–Pleistocene, are laid transgressively on these nappe units.

The southern sector, which includes the Serre and the Aspromonte Massifs, is formed by a series of nappes made up of granitic and metamorphic rocks, as well as by a sequence of arenaceous–conglomeratic and arenaceous–pelitic turbidites and varicoloured scaly clays, marls, limestones and sandstones with chaotic structure. Tortonian, Early Pliocene, and Upper Pliocene–

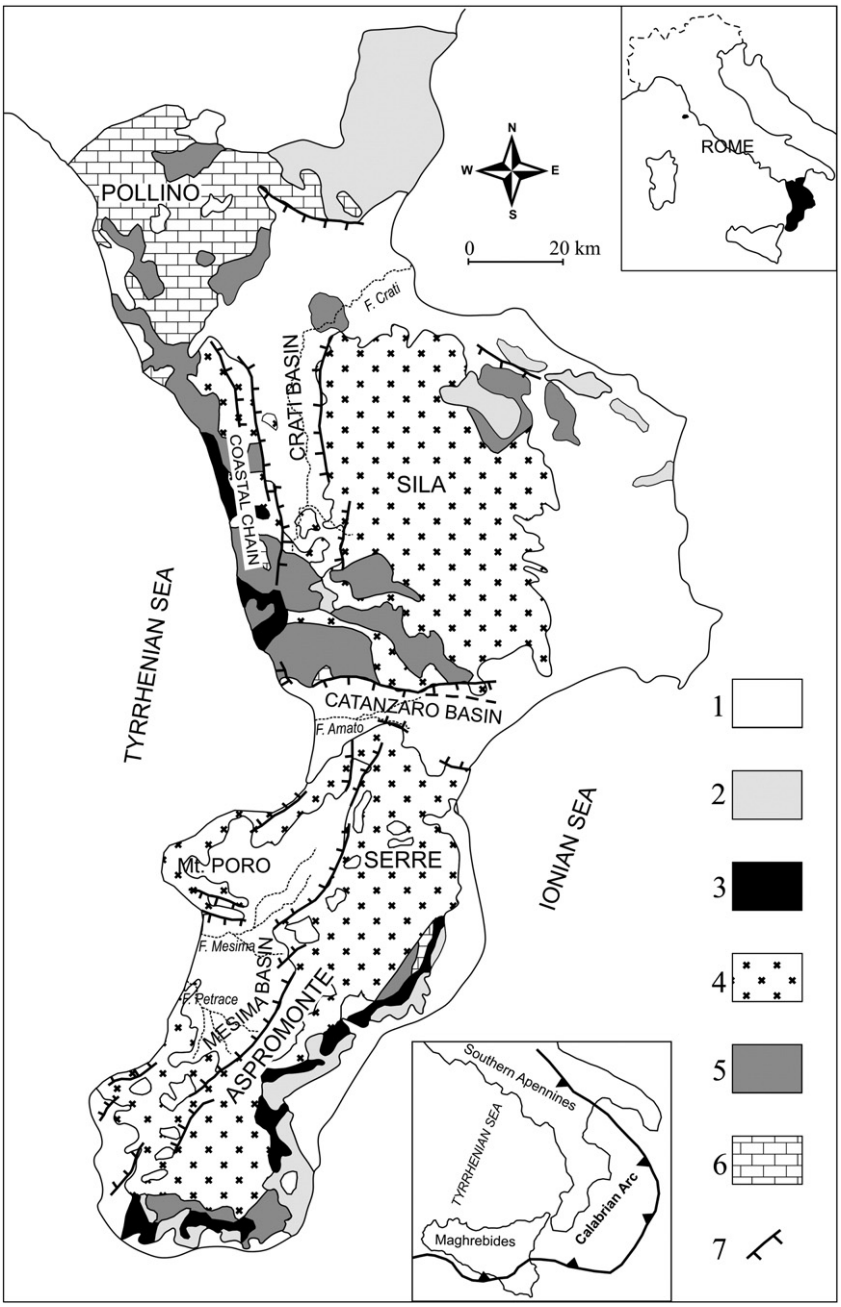

Fig. 1. Geological sketch of Calabria. Lithological units are grouped according to their mechanical behaviour. Legend: 1) Miocene to Holocene marine and continental sedimentary autochthonous units; 2) Mesozoic and Tertiary flysh–type sequences (they include Mesozoic quartzitic flysch of the NE Sila Massif, the Mesozoic–Tertiary flyschs of the NE Calabria, and Cretaceous–Oligocene varicolored shales); 3) Neogene hard sedimentary rocks (they were deposited in different sedimentary cycles); 4) Paleozoic medium- to high-grade metamorphic and intrusive rocks of the Alpine units derived from continental crust; 5) Paleozoic and Mesozoic very low to low-grade metamorphic rocks at places with ophiolites (they mainly belong to Alpine units derived by oceanic and continental crust and Appennine units); 6) Mesozoic–Paleogene carbonatic units of the Appennine Range and Mesozoic limestone cover of Alpine units in south Calabria; 7) Main morphotectonic structures. Modified from Sorriso-Valvo (1993).

Pleistocene sequences, made up of evaporitic and sedimentary rocks, overlap transgressively on this nappe building.

Although Calabria's rocks underwent several tectonic phases, the most ancient rocks were obviously exposed to greater deformation. This is particularly true for the crystalline–metamorphic rocks of the NW-verging EW-Alpine chain, which underwent two metamorphic events (Hercynian and Alpine orogeny). Moreover, the rapid regional uplift occurred during the Quaternary (average uplifting velocity 1 mm/yr), besides developing high relief energy caused significant fractures in the rocks. These events made crystalline–metamorphic rocks highly susceptible to deep weathering processes and, consequently, led to the formation of superficial soil covers prone to shallow landsliding.

From a morphological viewpoint, Calabria has a surface of about 15,075 km^2 with a prevalence of hills (49.2%) and mountains (41.8%), compared to lowlands (only 9%).

The lowland area is mainly represented by coastal plains; with the exception of the three major coastal plains of the main stream channels – in terms of length and discharge (Crati, Amato, Mesima and Petrace Rivers) – the majority of these plains lie parallel to the coast and are not very extended. These areas are characterized by clayey and silty–sandy deposits (Holocene–Pleistocene).

A substantial part of the territory is made up of hills, mainly developed on sedimentary deposits of the Upper Miocene–Pliocene and characterized by an overall gentle landscape, which however can be very rough because of the tendency of some terrains to develop badlands morphology. In general, the main processes of these areas are characterized by both shallow landslides and larger size landslides, as well as by erosion.

The mountainous part of the territory, characterized by steep acclivity and peaks over 1500 m asl, is represented by the Pollino Massif, the Coastal Chain, the Sila Massif, and the Serre–Aspromonte system (from north to south). These areas are essentially characterized by crystalline–metamorphic rocks where the weathering grade varies according to the outcropping lithotypes. The most widespread phenomena in this part of the territory are often large-sized landslides and deep-seated gravitational slope deformation (DGSD) (Sorriso-Valvo and Tansi, 1996).

Because of the orographic characteristics of the region (its elongated shape and the short distance between the main mountain systems and the sea), the hydrography (controlled by the major tectonic structures) displays a large number of basins of limited extension. Watercourses, generally developed over steep slopes and flowing on plains for very limited stretches, exert continuous erosion and undercutting of the slopes.

In general, the complex geological characteristics of the region, along with the strong seasonal contrast from a climatic viewpoint (Mediterranean climate) and the intense seismic and anthropic activity, all play a key role in making slopes prone to instability. In fact, landslides of small and large size as well as erosion processes are very common in this region. Recent unpublished studies carried out on wide sample areas allow us to estimate that about 20% of the regional territory is affected by landslide incidence; in regard to water soil erosion, about 2 mm/yr on average was estimated by ARSSA (2005).

2.2. Climate

Calabrian climate is Csa in Köppen's (1948) classification, with dry and hot summers and low average temperatures. The strong seasonal contrast is enhanced by rapid climate changes from one season to the other. In the dry season (April to September), rainfall represents 20–30% of the yearly total precipitation, about 1150 mm. The mean annual temperature ranges from 5 °C on the Pollino Range, with 10 °C on the mountain slopes to 18 °C along the coast. The average temperature in July is over 22 °C and rainfall may be 0. The maximum daily temperature may exceed 40 °C on some days in July and August. The average temperature in January is about 10 °C along the coasts and 4 °C in the mountains; above 1500 and 1700 m asl on the Sila and Aspromonte Massifs, respectively, the average temperature may frequently be below 0 °C. In summer, the temperature is more evenly distributed with values around 24 °C. All over Calabria, the temperature is linearly correlated with elevation, with an average gradient of −0.748 °C/hm on the Ionian side and −0.610 °C/hm on the Tyrrhenian side (Catani et al., 1995).

The precipitation regime is strongly influenced by the orography (Bellecci et al., 2002) from fronts transversally approaching the Calabrian peninsula and convective cells climbing up the steep seaside slopes of the mountain chains. In all seasons, low-pressure conditions cause intensive and long-lasting storms brought by warm air fronts approaching from the SE. In winter, extremely intense rainfalls are caused by cold air fronts approaching Calabria from the NW; in the short spring, the weather is highly unstable with lower rainfall; in summer, strong convective storms are frequent; and in autumn, intense precipitations are caused by cold air fronts that may approach from the NE.

In Fig. 2, the pattern of the pluviometric Angot coefficient (Pinna, 1977) is shown for the rain gauge stations in Calabria. The

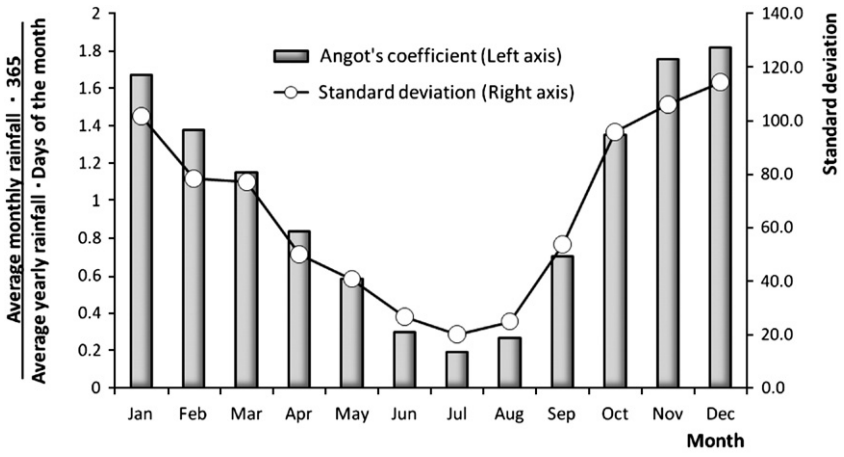

Fig. 2. Average values of the Angot's coefficients ($q=m/(P*n/365)$, where m=monthly rainfall, P=the annual rainfall and n=N° of days in a month), and standard deviations of the monthly rainfall relevant to the 313 rain gauge stations distributed in the Calabrian regional territory. The yearly rainfall, averaged and weighted over the regional territory and along the observation periods, is about 1076 mm.

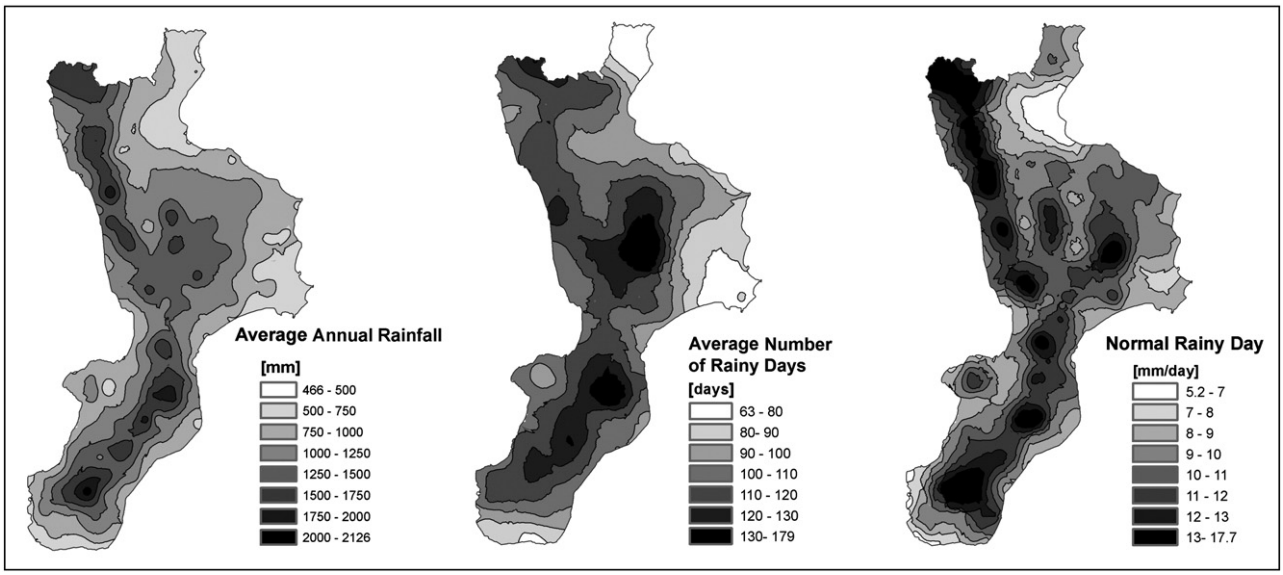

Fig. 3. Isocurves of the average annual rainfall, average number of rainy days, and of the normal rainy day for the Calabrian regional territory.

Angot coefficient is defined as $m/(P \cdot n/365)$, where m = monthly rainfall, P = yearly rainfall, and n = number of days in a month.

Yearly average rainfall is indeed >2000 mm on the Coastal Chain and the Aspromonte, whereas precipitation on the Ionian mountain slopes is between 600 and 1000 mm/yr, with values <500 mm/yr along the coastal plains.

Territorial distribution of the average annual rainfall, the average number of annual rainy days, and a "normal rainy day" i.e., the ratio between the two previous value, (Terranova, 2004a) is shown in Fig. 3.

A general frame of storm conditions in Calabria is provided by Versace et al. (1989) in order to define homogeneous zones and subzones of Calabria with regard to annual maxima of high-intensity and short-duration rainfalls [for a review see Terranova (2004b)]. Terranova (2004b) showed how events exceeding high thresholds, in terms of "normal rainy day," are more frequent on the Ionian side of Calabria.

3. Methodology

A high number of shallow landslides are triggered simultaneously, mostly by intense and short rainfall events. Considering the homogeneous distribution of pluviometric conditions over the territory, the occurrence of shallow landsliding phenomena on the same area largely depends on outcropping lithology. Susceptibility to shallow landslides on the same type of lithology depends on the presence of thicknesses (in some cases limited) of fresh or weak rocks (from very to intensely fractured) and/or soil covers of various origin (colluvium, residual soils, saprolitic soils, completely degraded/weathered rocks, etc.). The limited thickness of involved geomaterials (which is typical of the phenomena dealt with in this study) implies that modest volumes of geomaterials are involved in single shallow landslides, while rock volumes globally involved by shallow landslides as a whole and mobilized by a single rainfall event are often very large.

This study focuses on shallow landslides affecting different soil covers present on the various types of outcropped lithology in Calabria, which very often develop into fast mass movements, i.e., fast, shallow slide-flow instabilities. These phenomena involve limited soil cover thicknesses (~0.2 to 3.0 m). From a geometrical point of view, the phenomena are from 3 to 10 m wide and their total length depends on their evolution: once the event is triggered, it could either stop or develop into a debris flow or mud flow (Fig. 4).

Shallow instabilities as a whole, which are triggered by a specific rainfall event and that might develop into fast flow, are referred to in this paper as "shallow landsliding event." The rainfall event definition considered valid and used afterwards is "a sequence of rainy days preceded by and followed by at least one non-rainy day."

The methodology we propose aims at identifying susceptible areas and triggering scenarios of shallow landsliding events at a regional scale (Fig. 5). A database linked to a GIS has been created to support the proposed methodology in its various steps; the GIS are implemented by means of ArcGIS 9.0 package (ESRI, 2004). In particular, used informative layers refer to a digital terrain model, outcropping lithology, soils and land use, the maps of some significant shallow landslides of the past, and finally, rainfall related to these phenomena. Moreover, geotechnical characteristics of outcropping geomaterials have been carefully considered during the selection and calibration of predisposing factors.

In the first step, the distribution of predisposing factors of shallow instabilities has been evaluated at a regional scale. To this purpose, a map of the slopes has been drawn from the digital terrain model; two kinds of covers, prevalently coarse-grained (CG cover) or fine-grained (FG cover), have been identified, referring to the physical and mechanical characteristics of geomaterials and of the lithology map; soilscapes have been drawn from soil maps; and finally, the land use map has

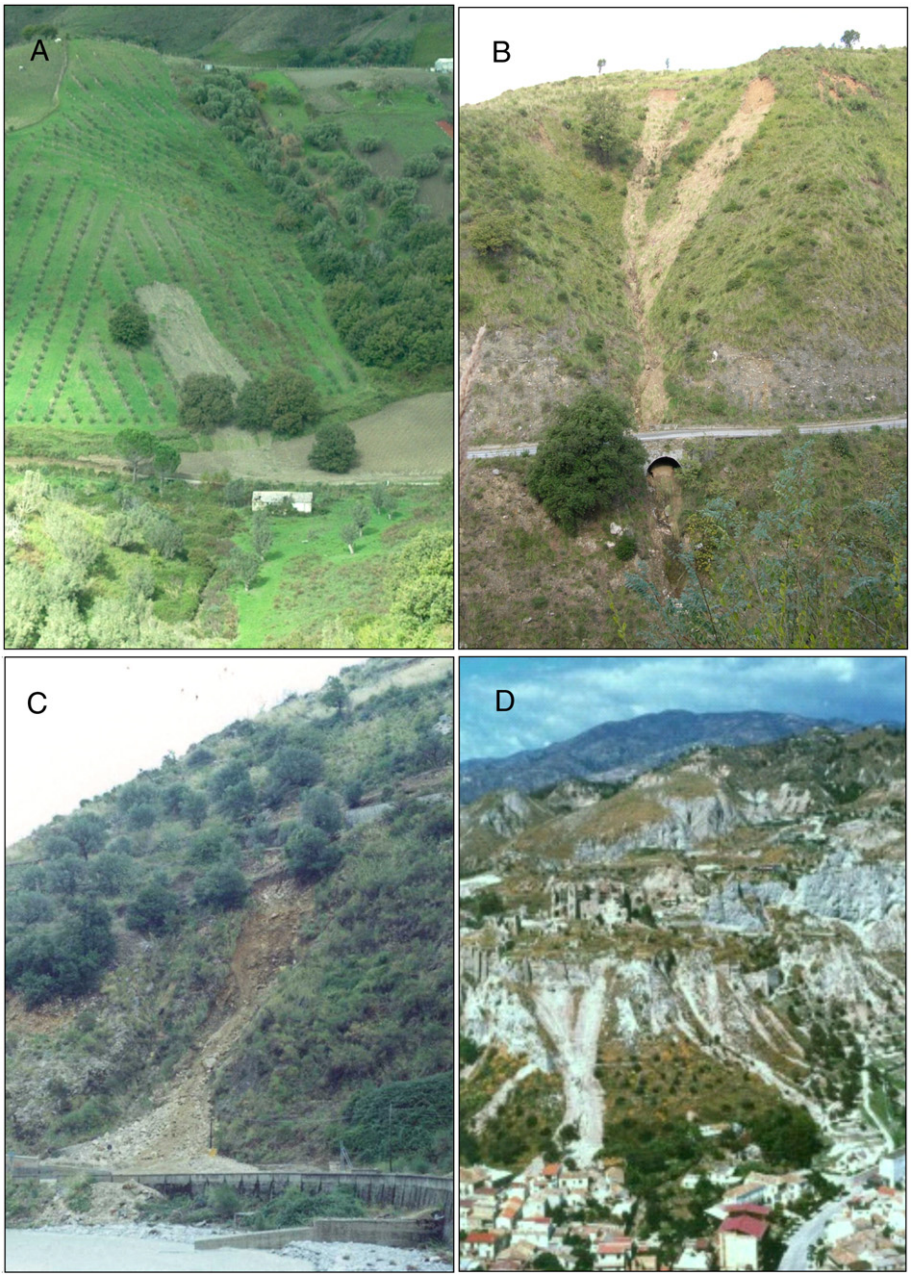

Fig. 4. Some typical shallow instabilities triggered by November 2004 meteorological event in central Calabria (A and B), and September 2000 meteorological event in southern Ionian Calabria (C and D).

been employed without any prior processing. Similarly, possible pluviometric triggering scenarios have been identified by jointly using the distribution over the territory of the factors characterizing rainfall events – such as maximum intensity and/or total rainfall and/or duration – and of shallow instabilities.

A statistical approach has been selected for this study because its focus was a specific type of landslide; this was also necessary to avoid using subjective criteria in evaluating the importance of the various predisposing factors from the scale of the study area as well as the type and quantity of available data. In particular, a simple multivariate statistical analysis method (Clerici et al., 2006), defined "Conditional Analysis Method," has been adopted. This approach enables us to evaluate susceptibility to shallow landsliding events according to the density of shallow instabilities and the various combinations of predisposing factors. Therefore, the importance of single predisposing factors for the susceptibility to shallow landsliding events is determined by this statistical approach, according to an objective criterion. In fact, the influence of predisposing factors is evaluated by overlapping the data contained in the maps of predisposing factors with the distribution of shallow landslides contained in the relevant informative layer. For example, by making reference to slope factor S, a number (Nc_S) of shallow landslides falling into a given slope class (c_S) and corresponding to the area $A(c_S)$ is calculated; this enables us to obtain the susceptibility density by means of the relation $\delta_S(c) = Nc_S / A(c_S)$.

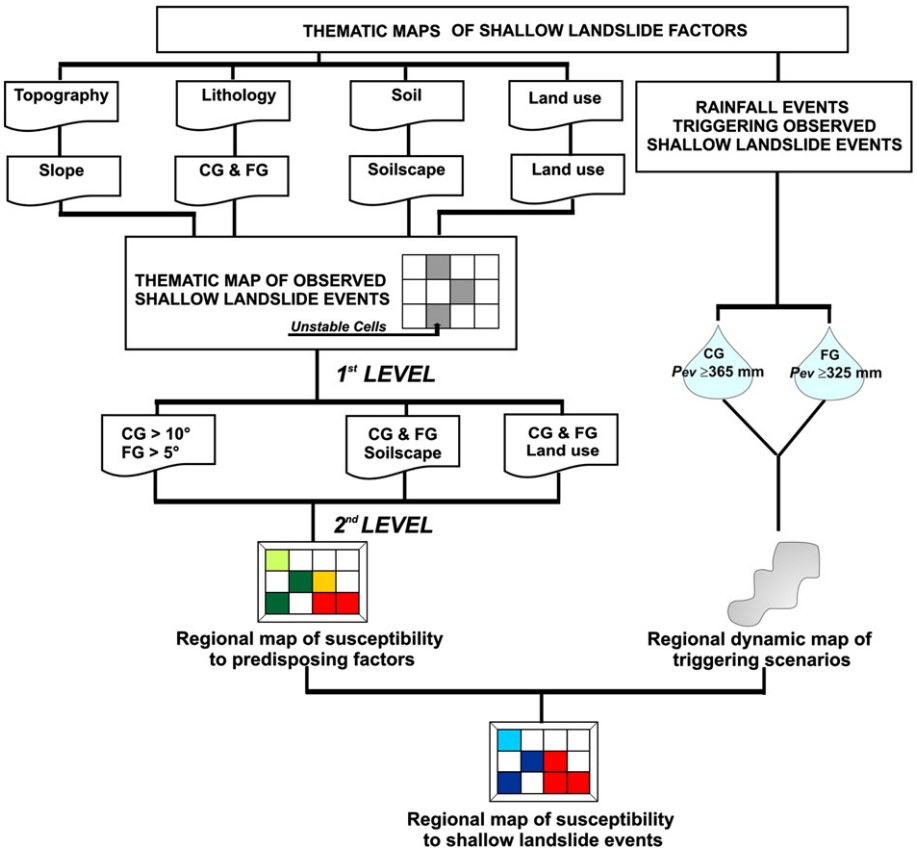

Fig. 5. Procedure used to identify and classify areas susceptible to shallow landsliding events at a regional scale. See text for a detailed explanation.

Therefore, the areas where $\delta_S(c)$ exceeds a given threshold value are considered susceptible to shallow landsliding events. In the same areas, the consistency of the possibility of developing shallow landslides must be tested; for example, when considering the slope factor, susceptibility of areas with flat, vertical, or subvertical slope might not be consistent with the physical process. In fact, geomaterials or geometrical conditions necessary for shallow landsliding events are usually not found in these kinds of slopes.

Given the scale and the aim of this study, a map of unstable cells (i.e., those cells where one or more shallow landslides are located) is drawn from the grid map of shallow landslides; moreover, counting of the landslides is carried out by making reference to the number of unstable cells.

In the first step, a first level susceptibility map is defined for each analysed factor; these maps are characterised by different susceptibility density values. Once these maps are crossed, they provide a second level susceptibility map characterised by a susceptibility density encompassing all the predisposing factors considered.

The diffusion of shallow instabilities in the susceptible areas, according to the second level study, will depend on the characteristics of rainfall events occurring in these areas.

For this reason, the methodology envisages the analysis to detect possible pluviometric scenarios that trigger shallow landslides. In order to identify these scenarios selecting one or more characteristics of the rainfall event and defining the relevant threshold values triggering shallow landsliding events are necessary. To this purpose, the methodology proposed focuses on shallow landsliding events and rainfall events strictly connected to them: one event identifies threshold values, while the others are useful to calibrate these threshold values. Since it is necessary to carefully document the events taken as a basis for the calibration (i.e., distribution of landslides and rainfalls in time and space), in this study researchers have been compelled to make use of only two events, that are however considered as very significant in terms of events extension and intensity.

4. Data collection

The data collected with the aim to characterize susceptible areas and triggering scenarios of shallow landslide events at a regional scale include slope angle (as DTM-derived map), lithology, soil and land use, maps of shallow landsliding events (carried out by means of detailed aerial photos interpretation and field survey), rainfall events related to shallow landsliding events and, finally, geotechnical features of covers. The predisposing factors were selected on the basis of their availability at regional scale, according to the data in the literature (among the others see Soeters and van Westen, 1996). Therefore, the analysis carried out provides a background of the location and extension of shallow landslides susceptible areas coherent at a regional scale; that is a fundamental pre-requisite to sharpen knowledge on susceptibility on a more detailed scale.

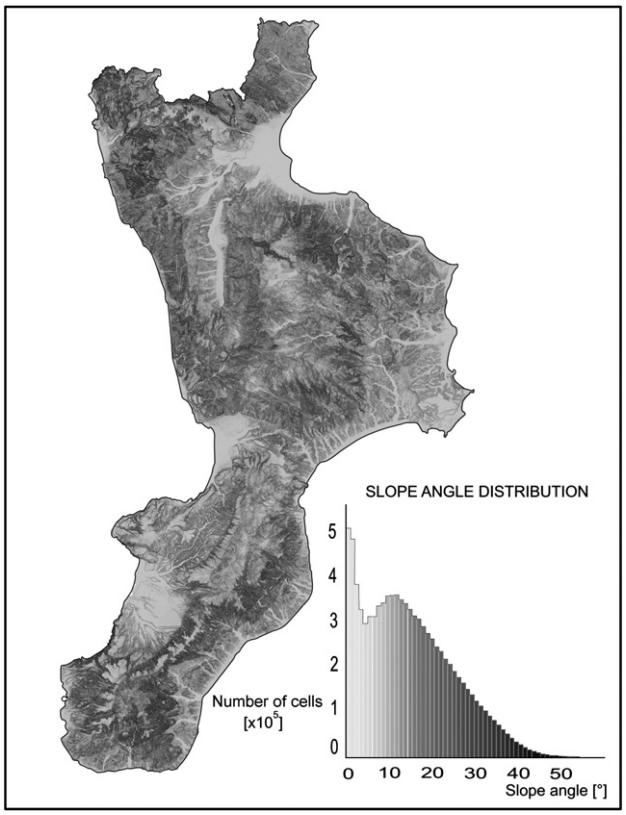

Fig. 6. Slope angle distribution of the Calabrian regional territory, i.e., the number of cells for each slope angle value.

4.1. Digital terrain model

In the investigation carried out within the framework of this study, a 40-m side square cell DTM has been employed. This size is generally greater than the size of the single shallow landslide, however, it is calibrated at a regional scale, which is the aim of this survey. To this purpose, the relation providing an estimate of the maximum slope value, which can be expected on average with the reduction of the cell size, has been statistically calculated. Statistical analysis has been carried out by looking for the relationships linking slopes reduction to the increasing cells size, by considering only a 40-m DTM. To this purpose, an area (1200 km^2 wide) located in that portion of the regional territory where shallow instabilities are mostly located, has been surveyed. This procedure statistically correlates the average values of maximum and average slope identified by means of variable cells size DTMs, created according to the 40-m DTM. Therefore, a DTM whose side was >40 m has been employed to reach a DTM whose side was 150 m. The statistical relationship obtained is subsequently extrapolated for a DTM whose side is <40 m. To sum up, the relationship found for the field of 40÷150 m DTMs is applied to the 10÷40 m DTMs. For example, by considering the size of investigated instabilities (about 10 m) and the slope of unstable cells for FG and CG covers (20° and 30°, respectively) when passing from a 40-m DTM to a 10-m DTM, maximum slope values of 28° and 47° (respectively) are obtained. The average approximation degree of the DTM employed in this study, as compared to the real situation, has been ultimately evaluated; this approximation degree grows worse with increasing slope.

Therefore, the necessary calculations have been made to detect the maximum slope value grid for each of the 9,433,581 cells making up the regional territory (Fig. 6). The distribution of the elementary frequency of slopes is bimodal and asymmetrical.

4.2. Lithology

Outcropping geological units of the region have been grouped according to the adopted map scale analysis and representation (1:250,000) in order to develop a lithotechnical map relevant to the covers. Two covers characterized by mechanical behaviour described as mainly frictional (CG cover) or mainly cohesive (FG cover) have been detected. The map of the two covers (Fig. 7) has been prepared by employing a progressive grouping of the above-mentioned geological units,

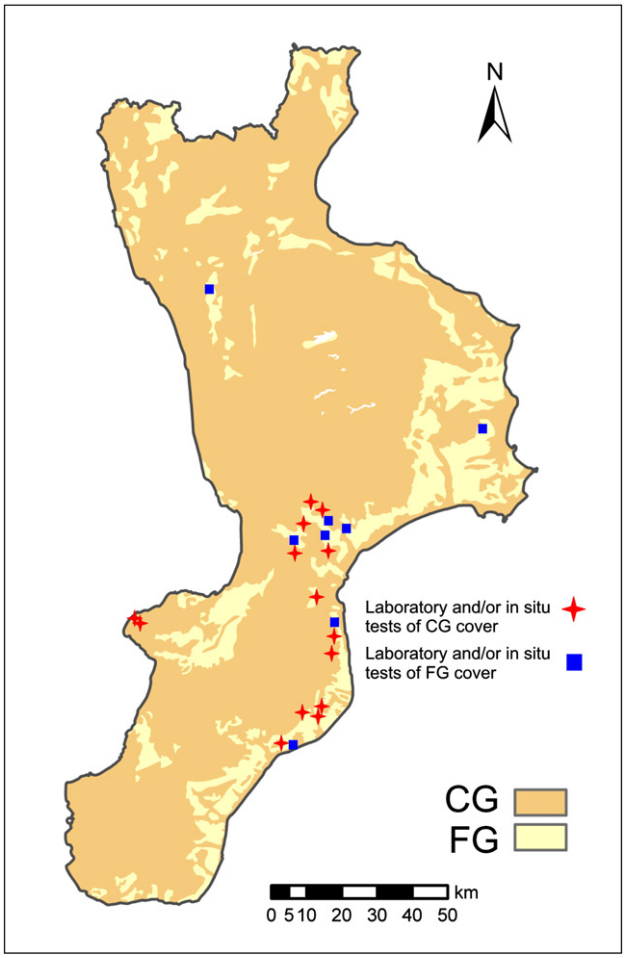

Fig. 7. Map of the two covers, coarse-grained (CG) and fine-grained (FG), prepared by employing progressive grouping of lithologic units characterized by similar mechanical behaviour. CG are the covers on the lithologic units represented by coarse-grained sediments (e.g., sandstones, conglomerates, etc.) and degraded and/or weathered crystalline–metamorphic rocks; FG are the covers on the lithologic units represented by fine-grained sediments (e.g., clay, silts, etc.).

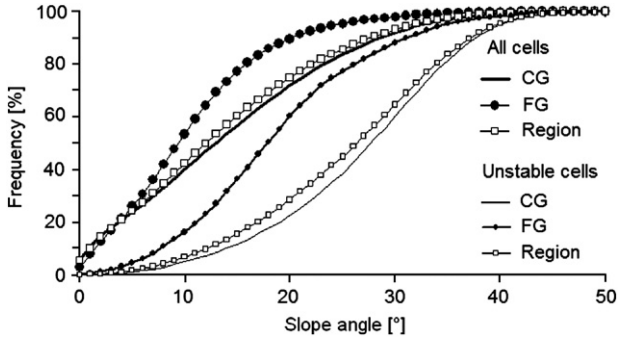

Fig. 8. Cumulative distribution function of the slope angles of the Calabrian region, relevant to all the cells and just to the unstable cells of the whole territory, the CG cover, and the FG cover.

according to observations and studies carried out in different areas of Calabria affected by shallow landsliding phenomena (Antronico et al., 2002, 2004). A clear prevalence of CG covers (about 82% of the regional territory) compared to FG covers (about 18%) was ultimately detected.

By crossing the CG and FG cover maps and the slopes map, the percentage distribution of the slopes relevant to CG and FG covers (Fig. 8) has been calculated. Slope distribution on CG covers is obviously very similar to the distribution over the whole regional territory, while slope distribution of areas with FG cover is more irregular. Moreover, elementary probability distribution frequency, which is not reported in Fig. 8, is characterised by two peaks.

4.3. Soil and land use

The great difference and spatial distribution of soil types in Calabria are a consequence of the mixed morphology of the territory, of its extremely complex geology producing a variety of lithological substrata (parent material), as well as of climate variability. As far as soils are concerned, a soil map of Calabria (scale 1:250,000) including 160 soilscapes, has been taken into account (ARSSA, 2003). The legend of the map lists the following: (i) for each soilscape, their inclusion in the Soil Region, the Soil Subregion, and the Great Soilscapes; (ii) the description of the soils constituting the association in a single map unit; (iii) the taxonomical classifications; (iv) the list of landscape elements (i.e., morphology, altitude, and slope); and (v) land capability maps (i.e., soil depth, texture, rockiness, drainage, etc.).

For this study, the research carried out also considers current land use (i.e., farmland, forestry use, etc.). Therefore, the Calabrian "land use map" has been derived from the processing of data inferred from the project *Corine Land Cover* (APAT, 2005) on a scale of 1:100,000, and whose legend includes 35 different land uses on three levels. The vast majority of the regional territory (56.1%) is represented by agricultural areas (olive groves and arable land), forests (broad-leaved and coniferous forests), and seminatural areas (transitional woodlands-shrub areas, as well as natural grassland) cover 33.8% and 7.6% of the regional territory, respectively.

Artificial surface and water bodies account for 2.4% and 0.1%, respectively, of the whole surface. Woodlands are very widespread and mostly present on mountains. Hills and plains are mainly used for agricultural purposes; cereals, and wine- and olive-growing are located on moderately steep slopes above all; and, valley bottoms are very often used for intensive farming.

4.4. Shallow landsliding events

Several shallow landsliding events have occurred in Calabria over the last 50 years. Table 1 summarizes some of the events that have been taken into consideration in this study.

The shallow landsliding event known as "*Central Southern Calabria 1951–1953*" and affecting a large part of the regional territory has been investigated by means of IGMI aerial photos dating back to 1954–1955. This event encompasses all the shallow landslides triggered by pluviometric events that hit central and southern Calabria in October and December 1951 and in October 1953 (Caloiero and Mercuri, 1980).

A second important landsliding event, named *"Catanzaro Isthmus 1985… 2004,"* includes shallow landslides triggered by heavy rainfalls affecting limited portions of the area of the Catanzaro Isthmus (central Calabria) in the periods indicated in Table 1 (Fig. 1). Also, this event encompasses a variety of landsliding events, and a map has been drawn after field surveys.

Although the landsliding event *"Mt. Poro 1998–1999–2002"* was the result of different landsliding events (triggered by rainfall events that occurred in December 1998, March 1999,

Table 1
Shallow landsliding events employed to make the inventory map

Reference area	Period	Methodology employed to map the shallow landslides	Number of unstable cells
Central Southern Calabria	1951 1953	1954–55 black and white aerial photos (1:33,000 approx. scale), 1:25,000 photo-restitution map of instabilities	22,777
Areas belonging to the Catanzaro Isthmus	March 1985 December 1987 March 1988 1989 March 1990 March 1996 May 1997 November 1997 April 2003 November 2004	Field surveys. Map of instabilities at 1:25,000 scale	509
Mt. Poro	December 1998 March 1999 April 2002	Field surveys. Map of instabilities at 1:50,000 scale	49
Southern Ionian Calabria	September 2000	Field surveys and aerial photo interpretation (1:25,000 approx. scale), 1:50,000 photo-restitution map of instabilities	3311

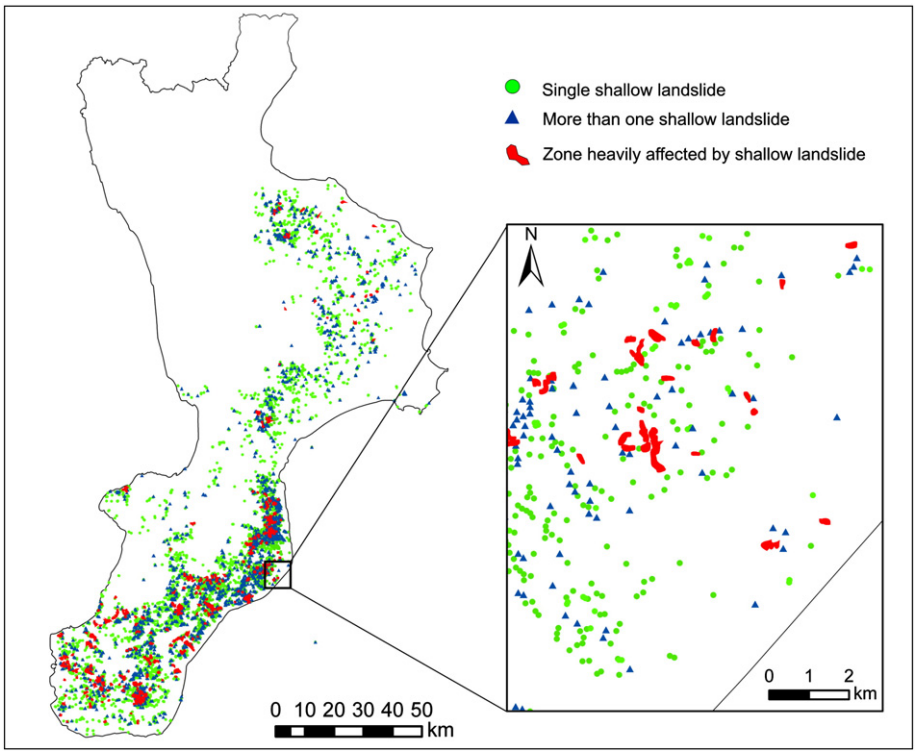

Fig. 9. Map relevant to the four shallow landsliding events that have been taken into consideration in this study. Green dot, single shallow landslides (these are isolated landslides that can be mapped individually); blue triangle, concentrated shallow landslides (although individually detectable by means of aerial photos and field surveys, they are too close to each other to be able to map them individually on the selected scale); red polygon, widespread shallow landslides (phenomena too close-set to be distinguished individually).

and April 2002), it affects a limited area. The areas affected by landsliding events, each made up of a limited number of shallow landslides, substantially coincide and are located on the terraced deposits facing the Tyrrhenian Sea in the NW area of Mt. Poro. Thanks to field surveys, we were able to draw a map of these shallow landslides.

The fourth surveyed landsliding event, named *"Southern Ionian Calabria 2000,"* was caused by shallow landslides triggered by precipitation that occurred in the southern Ionian part of Calabria between 8 and 10 September 2000 (Antronico et al., 2002; Sorriso-Valvo et al., 2004). Field surveys and photo-interpretation enabled the map to be drawn relevant to these shallow landslides.

The multi-temporal inventory map relevant to these four landsliding events is shown in Fig. 9.

Fig. 9 indicates that there are parts of the regional territory that are more prone to shallow instabilities. By using the slope map and the map relevant to the considered shallow landslides we were able to define the cumulative distribution frequency of unstable cells slopes for each event (Table 1 and Fig. 10).

4.5. Rainfall events

Rainfall events causing shallow landsliding events have been detected by using daily rainfall series. The choice of using daily rainfall series was because of the need to obtain rainfall data over longer periods of observation and common to a high number of rain gauges uniformly scattered over the territory. In particular, the data from 205 gauges (average gauge density: one over 75 km^2) stored in the database connected to the GIS used for the study have been employed.

As for the importance of rainfall data on a daily basis, although according to the common opinion single shallow landslides are triggered by rainfall accumulated in a short amount of time, a complete definition of shallow landsliding events (the number of shallow landslides and the areas where they occur) usually takes place in at least one or two days.

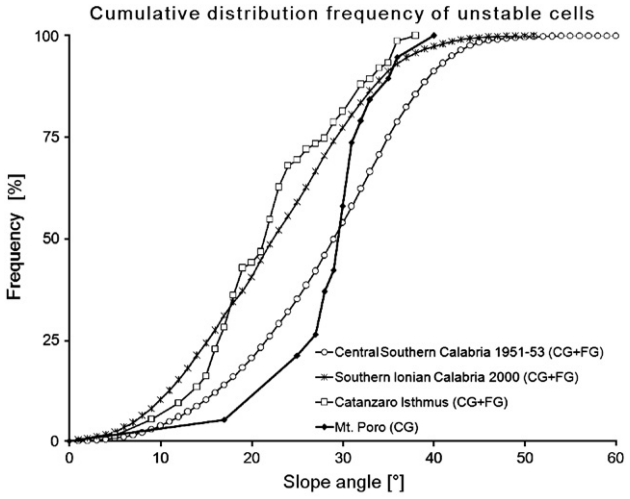

Fig. 10. Cumulative distribution frequency of unstable cells relevant to the shallow landslide events of the inventory map.

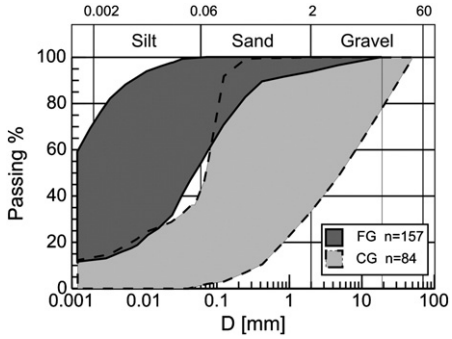

Fig. 11. Grain size distribution envelopes of fine-grained cover (FG) and coarse-grained cover (CG).

Among the typical features of a generic rainfall event, maximum intensity I_{max} i.e., the ratio between the peak rainfall and its duration, and total precipitation P_{ev} play a key role for the purpose of this study (Terranova and Gullà, 2004; Sorriso-Valvo et al., 2004; Terranova et al., 2007). By observing rainfall events in Calabria, we inferred that the values I_{max} and P_{ev} very frequently present similar areal distribution and, therefore, their simultaneous use is necessary only in a limited number of cases.

A hydrological survey has been carried out over the areas and dates of the shallow landsliding events listed in Table 1. For each considered landsliding event, the values of I_{max} and P_{ev} have been selected for each rain gauge. Iso-I_{max} and iso-P_{ev} maps at a regional scale have subsequently been created on the basis of these data by using kriging contouring procedures; these maps define rainfall events related to each considered shallow landslide event. The relevant maps represent other knowledge layers of analysis for subsequent observations.

4.6. Geotechnical features of covers

The geotechnical features of covers involved in shallow landslides affect two major aspects connected to landslides-triggering mechanisms and their evolution, i.e., (i) pore-water pressure and (ii) shear strength. To this purpose, geomaterials present in the areas affected by shallow landsliding phenomena have been tested in the laboratory and/or *in situ* (Fig. 7) (Cascini and Gullà, 1993; Gullà and Sorbino, 1994; Aceto et al., 1996; Antronico and Terranova, 1999; Antronico and Gullà, 2000; Antronico et al., 2002, 2004; Gullà et al., 2004a, 2006; Cascini et al., 2006). The reference framework of the physical and mechanical properties of geomaterials for FG and CG covers taken at a depth of 3 m or lower, is subsequently described.

Fig. 11 shows the envelopes containing the grain size distribution curves of FG and CG samples: 157 FG cover samples are taken from 8 sites and 84 CG cover samples are taken from 14 sites. Grain size distribution envelopes of the two covers are well differentiated; and in particular, FG covers are delimited by clay with silt and by slightly gravelly clayey silt with sand; CG covers are characterised by clayey sand with silt and by gravel with sand. As shown in Fig. 12, geomaterials in FG covers can be classified according to the Unified Soil Classification System (USCS) as inorganic clays of medium-

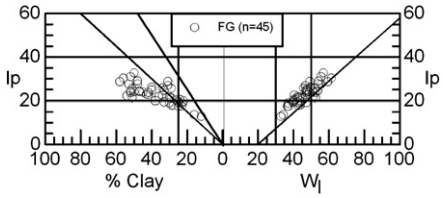

Fig. 12. Plasticity and activity charts of fine-grained cover (FG).

high plasticity characterized by medium and/or high plasticity and ranging from inactive to normally active (CL-CH).

By analyzing some of the main index properties, we may infer what has been indicated in Fig. 13, i.e., that the differences between FG and CG covers are significantly lower than that of the relevant grain size distribution envelopes. The amount of available experimental data is relevant (about 200 for FG and 100 for CG covers), and therefore, representative variation ranges for the considered properties can be identified.

As for geomaterials of FG covers, the following data have been found: the unit weight of solid particles varies from 25.7 kN/m^3 to 27.6 kN/m^3 (average value 26.6 kN/m^3); the unit weight of dry soil is included between 7.6 kN/m^3 and 17.2 kN/m^3 (average value 14.7 kN/m^3); the unit weight of natural soil varies from 10.0 kN/m^3 to 20.5 kN/m^3 (average value 18.3 kN/m^3); the unit weight of saturated soil varies from 14.7 kN/m^3 to 21.0 kN/m^3 (average value 19.3 kN/m^3); and finally, the void ratio varies from 0.54 to 2.06 (average value 0.84).

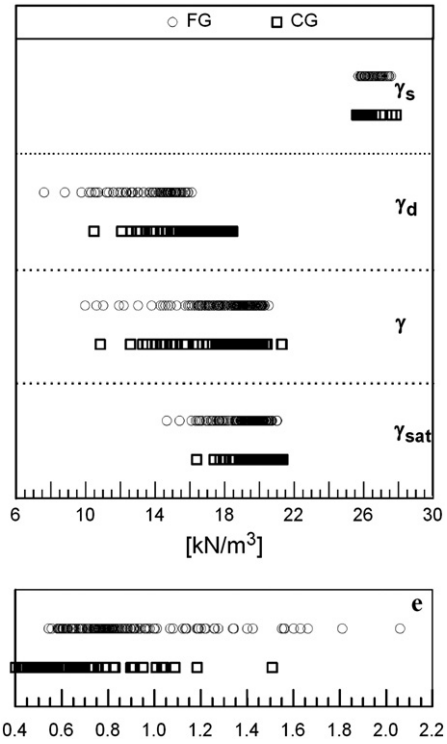

Fig. 13. Index property values of fine-grained cover (FG) and coarse-grained cover (CG): γ_s=unit weight of solid particles; γ_d=unit weight of dry soil; γ=unit weight of natural soil; γ_{sat}=unit weight of saturated soil; e=void ratio.

As for geomaterials of CG cover, the following has been found: the unit weight of solid particles varies from 25.6 kN/m^3 to 27.9 kN/m^3 (average value 26.2 kN/m^3); the unit weight of dry soil is included between 10.5 kN/m^3 and 18.5 kN/m^3 (average value 16.3 kN/m^3); the unit weight of natural soil varies from 10.8 kN/m^3 to 21.3 kN/m^3 (average value 18.1 kN/m^3); the unit weight of saturated soil is included between 16.4 kN/m^3 and 21.3 kN/m^3 (average value 20.0 kN/m^3); and finally, the void ratio varies from 0.40 to 1.51 (average value 0.62).

The fact that FG and CG covers are comparable is also supported by the study of permeability coefficient change intervals, as inferred from different techniques adopted *in situ* and in laboratory tests (Fig. 14). In particular, for FG covers, values range from 6.40×10^{-11} m/s to 1.62×10^{-2} m/s (average value 5.85×10^{-4} m/s); while CG values range from 3.45×10^{-9} m/s to 2.06×10^{-3} m/s (average value 1.68×10^{-4} m/s). Large range in the permeability is due at the lowest values that have been obtained in the geomaterials sampled, for example, on failure surfaces of shallow landslides, as compared to the values that have been obtained on degraded geomaterials involved in shallow landslides.

The indications obtained on the comparability of some physical characteristics of FG and CG covers surely deserve further research and can explain the fact that the same rainfall event might trigger shallow landsliding events affecting both FG and CG covers (Antronico et al., 2002; Gullà et al., 2004c; Sorriso-Valvo et al., 2004). Different densities of shallow instabilities detected as a consequence of the same rainfall event in these covers are mainly due to the different saturation mechanisms of FG and CG covers; these mechanisms have been experimentally pointed out for some case studies (Gullà and Sorbino, 1996; Gullà et al., 2004b).

In order to analyze the available data concerning the shear strength of geomaterials taken at a depth of up to 3 m from the ground surface, the potential triggering mechanisms of shallow landslides as well as the relative failure conditions have been examined (Gullà et al., 2004a, 2006): (i) as regards geomaterials affected by previous sliding phenomena, which have not evolved into flows, the residual shear strength or that included between the peak value and the residual value has been taken into consideration; (ii) as for geomaterials affected by seasonal and cyclical degradation processes, the shear strength of the artificially degraded geomaterials has been taken into account; (iii) for geomaterials accumulated on the slope by previous slide-flow landslides, the shear strength obtained by the reconstituted specimens from the same geomaterials has been considered. Shear strength parameters that have to be considered in these cases are those relevant to stress levels consistent with the thickness of the geomaterials involved in the instabilities.

By analyzing the data collected by Gullà et al. (2004a, 2006), Cascini and Gullà (1993), and because of further tests carried out in this study, the following friction angle values have been detected: for FG covers, peak friction angle varies from 31° to 65°; artificially degraded samples: from 19° to 42°; residual friction angle: from 16° to 36°; and friction angle relevant to reconstituted specimens: from 12° to 28°. For CG covers, peak friction angle varies from 40° to 60° and the residual friction angle from 30° to 48°. No indication concerning shear strength of artificially degraded and reconstituted specimens is available for CG covers. These indications, useful in completing the reference framework, are probably unessential for the study carried out at a regional scale, as shallow landslides in CG covers involving geomaterials accumulated on the slope by previous shallow landsliding phenomena can be considered as unimportant.

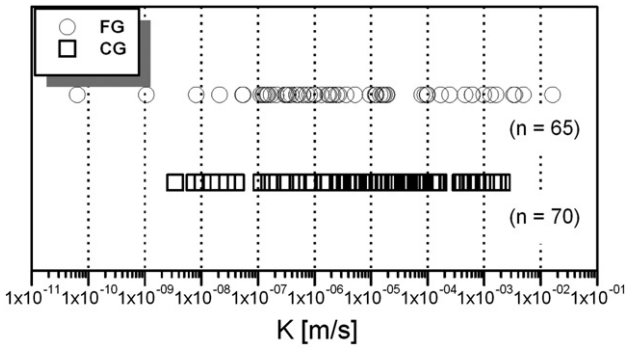

Fig. 14. Values of permeability coefficient obtained with *in situ* and laboratory tests for soils of the FG and CG covers.

According to what has been discussed so far regarding to the purpose of this study and the mechanisms that can trigger the studied landslides, potential friction angle values are included between 10–40° for FG covers and between 30–60° for CG covers. These intervals are a reference in the selection and calibration of predisposing factors for the shallow landsliding phenomena considered in this study, and they must be adjusted according to in-depth studies.

Further data concerning the typical conditions of geomaterials enabling shallow sliding phenomena to evolve into flows must be acquired. To this purpose, velocities must display values assumed as dangerous for people (Cruden and Varnes, 1996). As inferred from the results of the tests carried out by Gullà and Esposito (2003) on different soil–water mixtures of some geomaterials present in the surveyed areas, these velocities can be taken from the minimum slope values equal to 10–30° in FG covers and from 10–20° in the case of CG covers.

5. Survey

5.1. Strategy

The adopted strategy aims at progressively defining the areas prone to shallow landsliding events by making reference to the previously outlined general indications and available data.

The basic element of the procedure is the unstable cells map, obtained by the sum of the instabilities detected during previous studies carried out on the shallow landsliding events listed in Table 1. In particular, an unstable cell is a cell where one or more shallow landslides occur.

According to the available data, the classes c_S relevant to predisposing factors S are selected. Each class shall encompass

Table 2
Classification of susceptible areas in four classes

Cover	Class	Number of unstable cells	Area (km^2)	δ unstable cells/km^2
Coarse-grained (CG)	1	62	496.4	0.12
	2	1739	1779.4	0.98
	3	5524	1725.5	3.20
	4	13,496	1175.3	11.48
	2+3+4	20,759	4680	4.40
Fine-grained (FG)	1	2	39.4	0.05
	2	367	489.5	0.75
	3	1490	434.2	3.43
	4	2085	163.3	12.76
	2+3+4	3942	1087	3.60
Coarse- or fine-grained (CG+FG)	1	64	535.7	0.12
	2	2106	2268.8	0.93
	3	7014	2159.7	3.25
	4	15,581	1338.6	11.64
	2+3+4	24,701	5767	4.28

an area, $A(c_S)$, where a number of unstable cells, $N_{UNS}Ce$, are located. This area shall be defined on the basis of the unstable cells map. By using the previously outlined general definition, the density (δ) of unstable cells for each class of predisposing factor shall be calculated:

$$\delta = N_{UNS}Ce/A(c_S).$$

This ratio, which is always indicated for each class of predisposing factor, has been separately calculated for CG and FG covers.

By using this method, the importance of the classes of selected factors, thereby evaluating their efficacy, so as to define the susceptible area better, was detected.

5.2. Identification of susceptible areas

5.2.1. First level analysis

To define the areas susceptible to shallow landsliding events, cell minimum slope value (necessary for triggering shallow landslides) has been used as a first predisposing factor.

To choose reference values of cell slopes, the distribution of all cells and of unstable cell slopes has been compared at a regional scale and for the same area (Fig. 8), after they had been differentiated according to CG and FG covers.

Data shown in Fig. 8 and indications derived from available geotechnical data have provided the reference values (in the 40×40 m map) for slope threshold values of cells susceptible to shallow landslides. Calculations identified CG and FG cover cells, with slope values >10° and >5°, respectively, as susceptible to shallow instabilities.

The map obtained pinpoints the location of cells susceptible to shallow landsliding events and leads to the results shown in Table 3. At a regional scale, the initial area of 15,075 km^2 conventionally susceptible to shallow landsliding events is reduced by 34% to 9908 km^2. By considering the predisposing factor "unstable cells slope," we ultimately obtained the following unstable cells density: 2.71 unstable cells/km^2 in susceptible areas with CG cover and 2.01 unstable cells/km^2 in susceptible areas with CG cover.

The second predisposing factor employed to detect susceptible areas was the informative layer, derived from the "map soilscapes" inferred from the Soil Map (ARSSA, 2003).

A general examination of the areal distribution of unstable cells highlights their greater density in inland hilly areas and in the Ionian hilly side (characterised by moderately steep and steep slopes) and in the hilly and mountain areas of Sila, Serre, and Aspromonte (where steep and very steep slopes are present). The vast majority of stable cells are found in soilscapes characterised by plains and upland plains.

Fig. 15 shows unstable cells' densities and number calculated for those soilscapes displaying a density value >0.20 unstable cells/km^2.

Finally, the areas relevant to soilscapes for which the two following conditions have occurred contemporarily have not been considered as susceptible for shallow landsliding events. The two conditions are (i) a limited number of unstable cells (about 100), and (ii) limited unstable cells density values (<0.20 unstable cells/km^2).

The results obtained are shown in Table 3 with a density of 2.59 unstable cells/km^2 for CG and with a density of 2.15 unstable cells/km^2 for FG.

By means of the Soil Map (ARSSA, 2003), we calculated that the majority of unstable cells is located in soils with a >0.50-m thickness value; however, a significant presence of unstable cells was also detected in soilscapes where soil thickness was >0.20 and <0.50 m or even <0.20 m. This result – which has been proven by the surveys carried out on landsliding events that

Table 3
Synthesis of the first level analysis

Threshold values of predisposing factors	Cover	Susceptible area		Loss of unstable cells		δ
		km^2	%	Number	%	Unstable cells/km^2
Slope angle >10°	CG	7878	63	867	3.90	2.71
Slope angle > 5°	FG	2030	79	137	3.20	2.01
Soilscapes: $\delta \geq 0.20$ unstable cells/km^2 and $N_{UNS}Ce \geq 100$	CG	8561	69	60	0.27	2.59
	FG	1954	76	23	0.54	2.15
Land use: $\delta \geq 0.20$ unstable cells/km^2, $N_{UNS}Ce \geq 100$, and land use compatible with the occurrence of shallow landslides	CG	10,684	86	425	1.91	2.00
	FG	2285	89	76	1.80	1.81

The total area of the CG cover is equal to 12,433 km^2 with 22,221 unstable cells; the total area of the FG cover is equal to 2578 km^2 with 4230 unstable cells.

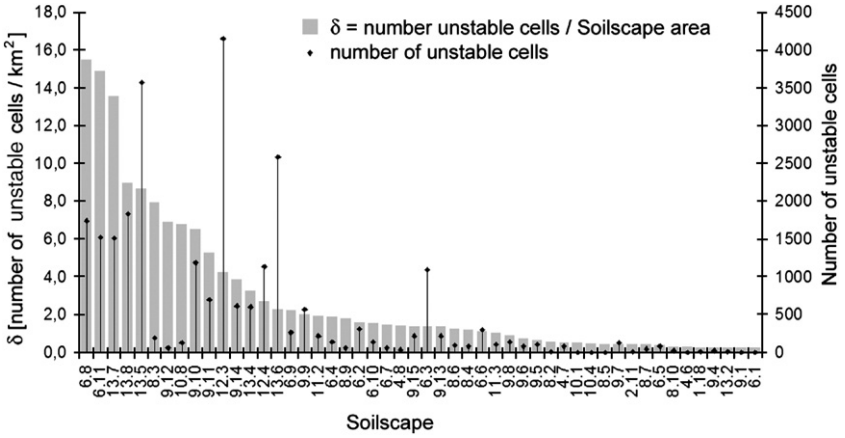

Fig. 15. Densities of the unstable cells and number calculated for those soilscapes displaying a density value >0.20 unstable cells/km^2. The codes on the horizontal axis correspond to those adopted in the ARSSA (2003) report. In particular, the soilscapes characterized by high (values are 6.8, 6.11, 13.7, 13.8, and 13.5. Classifications of the soilscapes drawn according to the USDA and WRB are the following: 6.8 — USDA: Typic Endoaquepts, fine loamy, mixed, thermic/Typic Endoaquepts, fine, mixed (calcareous), thermic; WRB: Hapli-Calcic Gleysols/Hapli-Gleyic Regosols. 6.11 — USDA: Typic Haploxerolls, loamy skeletal, mixed, thermic/Rock outcrop; WRB: Hapli-Skeletic Phaeozems. 13.7 — USDA: Humic Lithic Dystroxerepts, sandy, mixed, mesic/Typic Xerorthents, loamy skeletal, mixed mesic/Rock outcrop; WRB: Umbrihumic Leptosols (Dystric)/Hapli-Dystric Leptosols. 13.8 — USDA: Humic Lithic Dystroxerepts, sandy, skeletal, mixed, mesic/Rock outcrop; WRB: Areni-Leptic Umbrisols (Skeletic). 13.5 — USDA: Humic Dystroxerepts, sandy, mixed, mesic/Typic Xerorthents, loamy skeletal, mixed (non-acid), mesic/Rock outcrop; WRB: Endoskeleti-Humic Umbrisols/Hapli-Dystric Leptosols. Moreover, the soilscapes characterized by a high number of unstable cells are 12.3, 13.5, 13.6, 6.8, and 13.8. Classifications of the soilscapes drawn according to the USDA and WRB are the following: 12.3 — USDA: Humic Lithic Dystrudepts, coarse loamy, mixed, mesic/Humic Dystrudepts, coarse loamy, mixed, mesic/Rock outcrop; WRB: Umbrihumic Leptosols (Dystric)/Hapli-Humic Umbrisols. 13.6 — USDA: Humic Lithic Dystroxerepts, sandy skeletal, mixed, mesic/Typic Dystroxerepts, fine loamy, mixed, mesic/Rock outcrop; WRB: Areni-Leptic, Umbrisols (Skeletic)/Hapli-Dystric Cambisols.

occurred in Calabria (Antronico and Gullà, 2000; Antronico et al., 2004) – demonstrates that it is not recommendable to use soil thickness as a value to identify areas prone to shallow landsliding events.

The third predisposing factor employed to define the areas susceptible to shallow landsliding events was land use, as inferred by the Corine Land Use Map (APAT, 2005). The method used to detect cells susceptible to shallow landslides was to exclude those cells where land use is incompatible with shallow instabilities. To define susceptible areas, therefore, the distribution of the number of unstable cells according to the land use and their relevant density has been calculated; consequently, the cells where use is little affected by shallow instability events have been selected. Cell exclusion has been calculated so as to reduce the percentage loss of unstable cells. In particular, their exclusion depends on the contemporary check of the following conditions: limited number of unstable cells (about 100), limited unstable cell density (<0.20 unstable cells/km^2), and land use incompatible with the occurrence of shallow instabilities.

The results of cell selection carried out by means of the "land use" factor (Fig. 16) indicate a significant density of unstable cells in areas with the following land use: transitional woodland-shrub vegetation (3.2.4), bare rock (3.3.2), and sparsely vegetated areas (3.3.3). In the map used for this study, surfaces falling within the 3.3.2 category included areas surrounding river beds and, therefore, also the scarps of terraces where unstable cells relevant to this land use are located. From Fig. 16, we can also infer that a higher number of unstable cells are located in areas characterised by broad-leaved forests (3.1.1), coniferous forests (3.1.2), and olive groves (2.2.3). In particular, unstable cells falling within land use categories 3.1.1 and 3.1.2 are located near the secondary hydrographic network, where – due to the presence of incisions – woods are less thick.

The data on susceptible cells defined according to this method, are shown in Table 3. Density value of CG cover is 2.0 unstable cells/km^2, while the density of FG cover is 1.81 unstable cells/km^2.

Test checks carried out on well-known situations have highlighted that the limits in the employment of the land use factor in the location of susceptible areas are widely accepted for the analysis at a regional scale, and they generally imply the exclusion of flow deposit areas.

5.2.2. Second level analysis

The comparison of the results obtained for CG and FG covers by employing each single predisposing factor (slope, soilscape, and land use) can be carried out by defining susceptibility classes according to the density of unstable cells. Four different classes of susceptibility to shallow landslide events have been outlined: the first with $\delta<0.2$ unstable cells/km^2 density, the second with values ≥ 0.2 and <1.6, the third with ≥ 1.6 and <6.4, and the fourth with ≥ 6.4 density. As for susceptible areas located in the first level analysis and for both CG and FG covers, Figs. 17 and 18 indicate unstable cell distributions within the susceptibility classes obtained with the use of the three outlined factors (slope, land use, and soilscape). In particular, in terms of slope factor, four different slope classes have been defined by considering the modal value of the distribution of unstable cell frequency in the whole sample.

The employment of single factors (first level analysis), therefore, provides three different susceptibility maps. Second

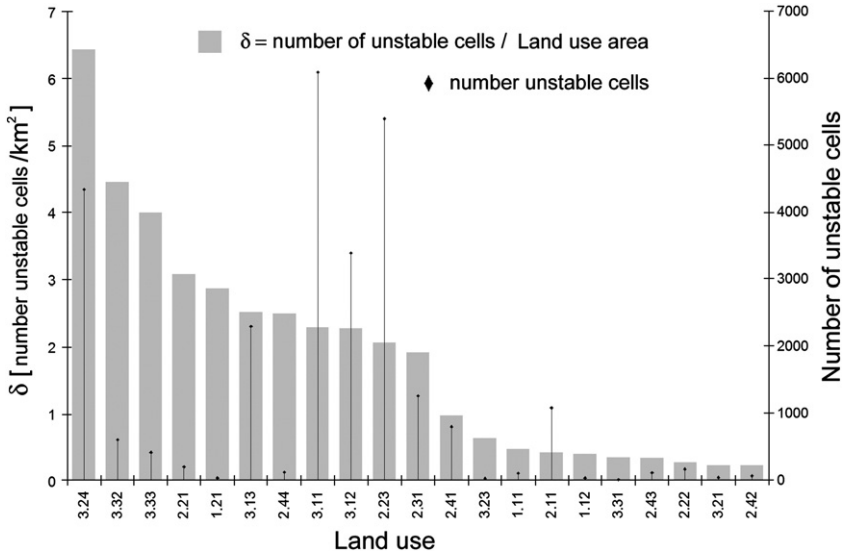

Fig. 16. Densities of the unstable cells and number calculated for those land use map units displaying a density value >0.20 unstable cells/km^2. The codes on the horizontal axis correspond to those adopted in the Corine Land Cover Report (APAT, 2005).

level analysis, however, enables better location of areas susceptible to shallow landsliding events by means of the crossing of the three susceptibility maps.

In such a map, we were able to calculate the density of unstable cells in each crossing area and to assign a relevant susceptibility class to each cell (Fig. 19). Second level analysis pinpoints a total area of 6303 km^2 with various susceptibility classes to shallow landsliding events, where 24,765 unstable cells are located (20,821 unstable cells in 5176 km^2 with CG cover and 3944 unstable cells in 1126 km^2 with FG cover). The employed procedure therefore excludes an area of 8714 km^2 at a regional scale; 55% of this area corresponds to CG covers, and 45% corresponds to FG covers. A very low level of susceptibility to shallow landsliding events is calculated to the excluded area; however, susceptibility is not zero because no density values or shallow landslides number exceeding a certain threshold are attributed to the three predisposing factors considered simultaneously.

In the area encompassing the three highest susceptibility classes (classes 2, 3, and 4), the data summed up in Table 2 highlight that a value δ=4.4 unstable cells/km^2 for CG cover, compared to an initial value of 1.79 unstable cells/km^2 for the whole regional CG area, and a value δ=3.6 unstable cells/km^2 for FG covers, compared to an initial value of 1.64 unstable cells/km^2, are present. Finally, if we consider the whole regional territory and the highest susceptibility class, an area of 1339 km^2 is identified with δ=11.64 unstable cells/km^2.

5.3. Identification of triggering scenarios

In the area described as susceptible to shallow landsliding events, the size of the areas that could be affected by these phenomena will depend on the characteristics of rainfall events. To this purpose, an analysis has been carried out to select rainfall scenarios able to trigger shallow landsliding events. Daily rainfall series, relevant to the 205 rain gauges scattered over the regional territory, have therefore been employed; one or more characteristics of rainfall events have been selected.

According to what has been previously stated about the shallow landsliding events and the relevant rainfall events, two main characteristics of the rainfall event have been chosen: rainfall maximum intensity, I_{max}, and total rainfall, P_{ev}. The analyses carried out in previous studies in Calabria (Antronico et al., 2002; Sorriso-Valvo et al., 2004; Terranova et al., 2007) have highlighted that I_{max} and P_{ev} are the two triggering factors that mostly contribute to shallow landsliding events.

The first step of the analysis, separately carried out for CG and FG covers, is aimed at selecting the threshold values for I_{max} or P_{ev} typical of a rainfall event able to trigger shallow

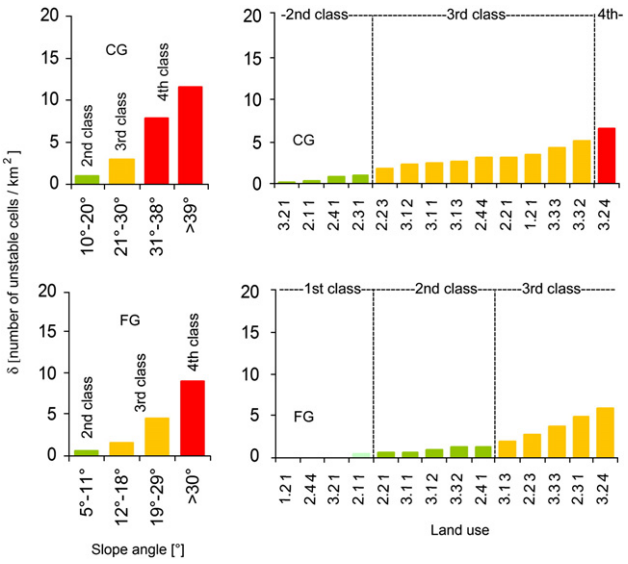

Fig. 17. Unstable cell distributions within the susceptibility classes obtained with the use of the slope and land use parameters. With reference to land use, the codes on the horizontal axis correspond to those adopted in the Corine Land Cover Report (APAT, 2005).

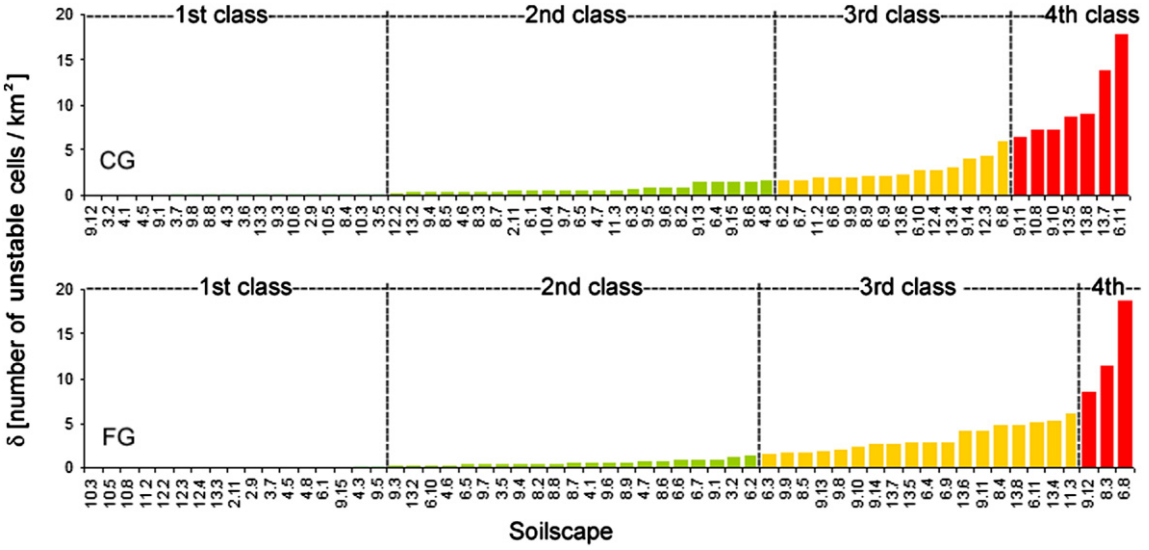

Fig. 18. Unstable cell distributions within the susceptibility classes obtained with the use of the soil predisposing factor. The codes on the horizontal axis correspond to those adopted in the ARSSA (2003) report. For the fourth susceptibility class of the CG covers, the classifications according to the USDA and WRB methodology are the following: 6.11 — USDA: Typic haploxerolls, loamy skeletal, mixed, thermic/Rock outcrop; WRB: Hapli-Skeletic Phaeozems. 13.7 — USDA: Humic Lithic Dystroxerepts, sandy, mixed, mesic/Typic Xerorthents, loamy skeletal, mixed mesic/Rock outcrop; WRB: Umbrihumic Leptosols (Dystric)/Hapli-Dystric Leptosols. 13.8 — USDA: Humic Lithic Dystroxerepts, sandy, skeletal, mixed, mesic/Rock outcrop; WRB: Areni-Leptic Umbrisols (Skeletic). 13.5 — USDA: Humic Dystroxerepts, sandy, mixed, mesic/Typic Xerorthents, loamy skeletal, mixed (non-acid), mesic/Rock outcrop; WRB: Endoskeleti-Humic Umbrisols/Hapli-Dystric Leptosols. 9.10 — USDA: Lithic Xerorthents, coarse loamy, mixed (calcareous), mesic/Rock outcrop; WRB: Hapli-Calcaric Leptosols. 10.8 — USDA: Typic Xerorthents, coarse loamy, mixed, thermic/Rock outcrop; WRB: Hapli-Dystric Leptosols. 9.11 — USDA: Vertic Eutrudepts, fine loamy, mixed, mesic — Aquic Eutrudepts, fine, mixed, mesic; WRB: Hapli-Calcaric Cambisols- Haplic Calcisols. For the fourth susceptibility class of the FG covers, the classifications according to the USDA and WRB methodology are the following: 6.8 — USDA: Typic Endoaquepts, fine loamy, mixed, thermic/Typic Endoaquepts, fine, mixed (calcareous), thermic; WRB: Hapli-Calcic Gleysols/Hapli-Gleyic Regosols). 8.3 — USDA: Fluventic Haploxerepts, coarse loamy, mixed, thermic; WRB — Eutri-Fluvic Cambisols. 9.12 — USDA: Typic Xerorthents, fine, mixed (calcareous), mesic; WRB — Calcari-hyposodic Regosols.

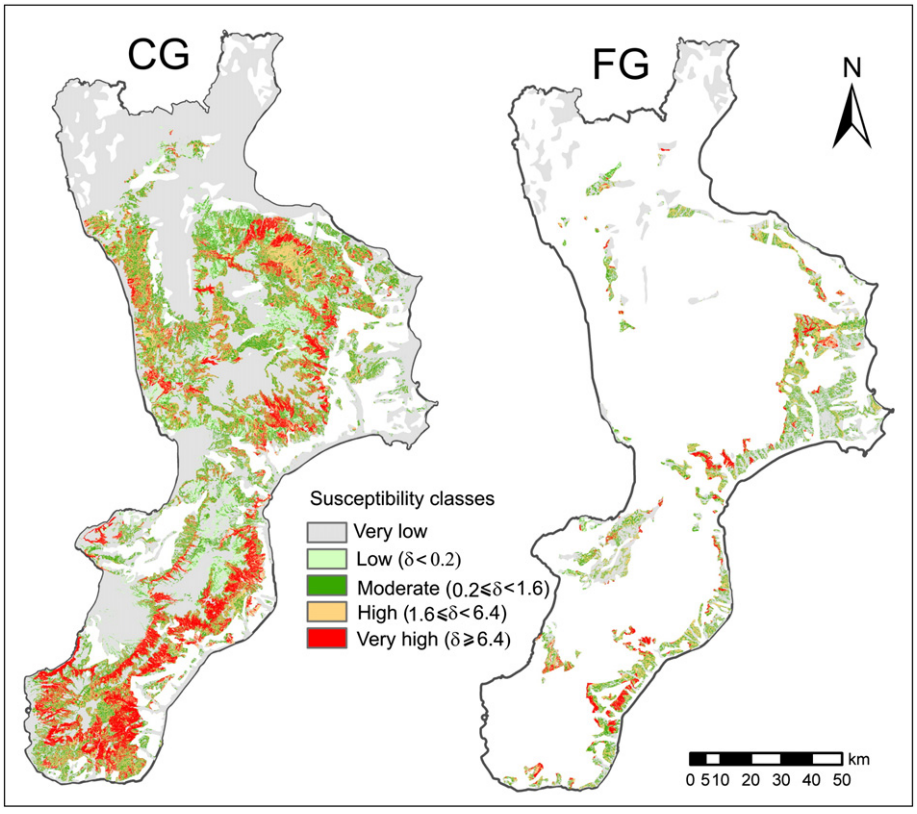

Fig. 19. Second level map of susceptibility to predisposing factors relevant to CG covers (left) and to FG covers (right).

Table 4
Rainfall thresholds determination to delineate the pluviometric scenarios on the CG and FG covers

	Southern Ionian Calabria 2000	Central Southern Calabria 1951–53		
	Rainfall threshold based on 95% of unstable cells enveloped	% of unstable cells enveloped		
		15 October 1951	30 December 1951	20 October 1953
P_{ev}(CG) (mm)	365	78	0	79.5
P_{ev}(FG) (mm)	325	78.7	0	89.3
I_{max}(CG) (mm/d)	170	71	0	34
I_{max}(FG) (mm/d)	158	79	0.3	62

landslides. To this purpose, the rainfall event related to the shallow landsliding event defined as "*Southern Ionian Calabria 2000*" has been selected for the following reasons: (i) there is a better relation between shallow landsliding event and rainfall event; (ii) the shallow landsliding event is better characterised in terms of number of shallow landslides and their location; and (iii) CG and FG covers in the area, as well as the interval of the slopes affected by shallow instabilities, are well represented.

According to the procedure, once the rainfall event has been selected, the isocurve of a generic function of I_{max} or P_{ev}, including a high percentage of unstable cells of the relevant shallow landsliding event, must be selected.

Rainfall events pointed out by means of this method can be compared to other known and well-documented landsliding events along with their relevant rainfall events. In case these tests do not produce satisfactory results, the procedure continues with a different threshold value.

In this study, tests have been carried out defining the areas affected by the five rainfall events triggering the shallow landsliding events named "*Central Southern Calabria 1951–1953*".

Table 4 indicates the threshold values of P_{ev} and I_{max} – for both CG and FG values – obtained by the relevant isocurves, including 95% of the unstable cells of the *"Southern Ionian Calabria 2000"* shallow landsliding event. Table 4 also reports the percentage of unstable cells of the event "*Central Southern Calabria 1951–53*," delineated by using three rainfall events out of five (15 October 1951, 30 December 1951, 20 October 1953) exceeding the threshold values. Fig. 20A shows the map of the areas (differentiated according to the CG and FG covers) relevant to P_{ev} threshold values and encompassing about 95% of the unstable cells of the event "*Southern Ionian Calabria 2000.*" By employing pre-set threshold values (P_{ev}=365 mm for CG and 325 mm for FG), the map was drawn (Fig. 20B)

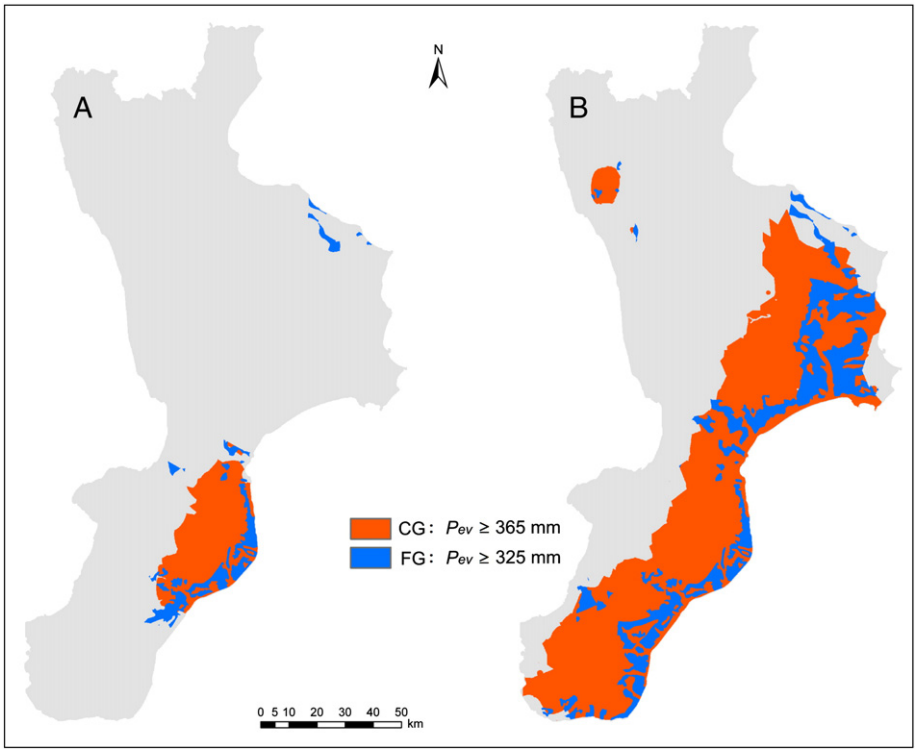

Fig. 20. Pluviometric scenarios triggering the shallow landsliding events occurred in southern Ionian Calabria in September 2000 (A) and in central southern Calabria in 1951 and 1953 (B).

relevant to the event named *"Central Southern Calabria 1951–53,"* encompassing over 78% of unstable cells.

The study carried out shows that (at a regional scale) rainfall events able to trigger shallow landsliding events are assessed by using the following values: $P_{ev} \geq 365$ mm for CG covers and $P_{ev} \geq 325$ mm for FG covers. These rainfall scenarios are further defined by jointly using the values $I_{max} \geq 170$ mm for CG and $I_{max} \geq 158$ mm for FG covers.

6. Discussion

Second level analysis enabled us to identify and classify areas susceptible to shallow landsliding events at a regional scale (Fig. 19).

For a given rainfall event, by using the threshold values identified for P_{ev} and I_{max}, the relevant pluviometric scenario can be delineated; and therefore, the area (at a regional scale) where the shallow landsliding event related to rainfall will most likely occur can be defined.

What we have described so far concerns (i) a precipitation event of the past characterized by P_{ev} and/or I_{max} values of given probability, to which no shallow landsliding event is related; (ii) a rainfall event where connection with a shallow landsliding event is well documented; and (iii) an ongoing rainfall event that could become highly critical for a shallow landsliding event.

The results obtained in the first case (area considered as susceptible to a potential shallow event at a regional scale) can also be employed to carry out historical surveys with the aim of documenting shallow landsliding events unknown so far. According to the results of the historical survey, the model can be adjusted by means of the analysis carried out in this study for better identification of susceptible areas at a regional scale and by means of the relevant rainfall scenario. For example, over the 50 year period running from 1951 to 2000, 42 rainfall events with $P_{ev} > 325$ mm (and with various territorial extensions) as well as 40 rainfall events with $P_{ev} > 365$ mm have been detected; therefore, targeted historical surveys can be carried out focusing on the previously mentioned dates.

Analyses that can be carried out in the second and third mentioned cases may test the coherence of the results obtained by the *a posteriori* simulation, or the forecasting simulation, thanks to different approaches. Simulation results can be considered coherent when the area considered as susceptible encompasses a number of unstable cells for pre-set P_{ev} and/or I_{max} values higher than the threshold values applied to the simulation. If, during the simulation of a given rainfall event, statistically significant incoherent results are obtained, the model must be adjusted according to the following procedure: (i) no shallow instabilities are found in a susceptible cell located in the triggering scenario area → the importance of predisposing factors shall be increased and/or threshold values for P_{ev} and/or I_{max} shall be reduced; (ii) shallow instabilities are detected in a susceptible cell located outside the triggering scenario area → P_{ev} and/or I_{max} threshold values shall be reduced; (iii) shallow instabilities are detected in a non-susceptible cell within the boundaries of the triggering scenario area → the importance of the predisposing factors shall be increased; and (iv) shallow instabilities are detected in a non-susceptible cell located outside the triggering scenario area → the importance of predisposing factors and/or P_{ev} and/or I_{max} threshold values shall be reduced.

7. Conclusion

The work carried out so far enabled us to pinpoint different susceptible areas to shallow landsliding events on natural slopes at a regional scale. Moreover, daily rainfall threshold values (P_{ev} and/or I_{max}) have been detected and may be helpful in identifying the relevant triggering scenario for potential shallow landsliding events for a given rainfall occurrence.

Obtained results can be employed to manage emergency situations at a regional scale for shallow landsliding events triggered by intense rainfalls, thereby defining different alert levels. Data collected systematically in the management of emergency situations and employed in the procedure described so far will enable us to detect the susceptible areas and to improve the reliability of intense rainfall scenarios.

A definition of the areas at a regional level, classified according to the different susceptibility classes, enabled researchers to select suitable areas and sites to study triggering mechanisms of shallow instabilities and their evolution. Thanks to the data acquired, we were able to detect shallow instabilities in geologically homogenous areas (shallow landslides in fine-grained, in coarse-grained, and in weathered soils, etc.). To this purpose, it would be useful to have better areal or time data concerning rainfall or its integration with data on positive and negative pore pressure in those areas where shallow landsliding phenomena are more frequent (Gullà and Sorbino, 1996; Gullà et al., 2004b).

The methodology we propose in this study aims at risk mitigation and prevention actions in a specific area. Moreover, by integrating the analyses carried out and the detailed surveys on single areas affected by shallow landslides, further progress is expected to develop more efficient methodologies to plan and implement measures for risk mitigations and reduction, which – as everybody knows – are normally extremely complex and expensive.

Acknowledgments

The authors are very grateful to the anonymous referees and to the editor for their constructive comments. The authors express their gratitude to Luigi Borrelli (CNR-IRPI) for his valuable assistance in the analysis of geological data.

References

Aceto, L., Gullà, G., Sorbino, G., 1996. Caratterizzazione geotecnica delle argille affioranti nel bacino del Torrente Turbolo (Calabria settentrionale) (Progress Report 1). Tecnical Report, vol. 478. CNR IRPI, Cosenza, Italy. 30 pp.

Aleotti, P., Chowdhury, R., 1999. Landslide hazard assessment: summary review and new perspectives. Bulletin of Engineering Geology and the Environment 58, 21–44.

Aleotti, P., Baldelli, P., Polloni, G., 1996. Landsliding and flooding event triggered by heavy rains in the Tanaro Basin (Italy). Proceedings of the International Symposium Interpraevent, 24–28 June 1996, Garmisch-Partenkirchen, Germany. Bayerisches Landesamt für Wasserwirtschaft, pp. 377–386. D.

Amodio-Morelli, L., Bonardi, G., Colonna, V., Dietrich, D., Giunta, G., Ippolito, F., Liguori, V., Lorenzoni, S., Paglionico, A., Perrone, V., Piccarreta, G., Russo, M., Scandone, P., Zanettin-Lorenzoni, E., Zuppetta, A., 1976. L'Arco Calabro Peloritano nell'Orogene Appenninico-Magrebide. Memorie della Società Geologica Italiana 17, 1–60.

Antronico, L., Gullà, G., 2000. Slopes affected by soil slips: validation of an evolutive model. Proceedings of the VIII International Symposium on Landslides — Landslide in Research, Theory and Practice, 26–30 June 2000, Cardiff, Wales. Thomas Telford, London, UK, pp. 77–84.

Antronico, L., Terranova, O., 1999. Indagine sull'erosione e sulla capacità d'infiltrazione mediante piogge simulate. GEAM. Geoingegneria Ambientale e Mineraria 23, 135–141.

Antronico, L., Gullà, G., Terranova, O., 2002. L'evento pluviometrico dell'8-10 settembre 2000 nella Calabria Ionica meridionale: dissesti sui versanti e processi in alveo. Proceedings of the Conference Il Dissesto Idrogeologico: Inventario e Prospettive, 5 June 2001, Rome, Italy. Accademia Nazionale dei Lincei, Rome, Italy, pp. 67–79.

Antronico, L., Gullà, G., Borrelli, L., 2004. Shallow instabilities for sliding flow: regional influence and area affects. Proceedings of the IX International Symposium on Landslides, 28 June-7 July 2004, Rio de Janeiro, Brasil. A.A. Balkema, Rotterdam, The Netherlands, pp. 1381–1387.

APAT, 2005. Project: Corine Land Cover 2000 Italy. Report 36/2005, Agenzia per la Protezione dell'Ambiente e per i Servizi Tecnici. 86 pp.

ARSSA, 2003. I suoli della Calabria - Carta dei suoli in scala 1:250,000 della Regione Calabria. ARSSA, Agenzia Regionale per lo Sviluppo e per i Servizi in Agricoltura, Settore Servizi Tecnici di Supporto, Servizio Agropedologia, Monografia divulgativa. Rubbettino Publisher, Soveria Mannelli, Italy, 387 pp.

ARSSA, 2005. Carta del rischio di erosione attuale e potenziale della regione Calabria. Scala 1:250,000. ARSSA, Agenzia Regionale per lo Sviluppo e per i Servizi in Agricoltura, Settore Servizi Tecnici di Supporto, Servizio Agropedologia, Monografia divulgativa. Editrice Cerbone, Napoli, Italy, 107 pp.

Bellecci, C., Federico, S., Casella, G., Avolio, E., Lo Feudo, T., Sisca, M., 2002. Intense Precipitation in southern Italy. In: Gaudio, R. (Ed.), New Trends in Hydrology. Editoriale BIOS, Cosenza, Italy, pp. 57–74.

Bonardi, G., De Vivo, B., Giunta, G., Lima, A., Perrone, V., Zuppetta, A., 1982. Mineralizzazioni dell'Arco Calabro-Peloritano. Ipotesi genetiche e quadro evolutivo. Bollettino della Società Geologica Italiana 101, 141–155.

Caloiero, D., Mercuri, T., 1980. Le alluvioni in Calabria dal 1921 al 1970. Geodata, vol. 7. CNR IRPI, Cosenza, Italy. 161 pp.

Can, T., Nefeslioglu, H.A., Gokceoglu, C., Sonmez, H., Duman, T.Y., 2005. Susceptibility assessments of shallow earthflows triggered by heavy rainfall at three catchments by logistic regression. Geomorphology 72 (1–4), 250–271.

Carrara, A., Guzzetti, F., 1995. Geographical Information Systems in Assessing Natural Hazards. Kluwer Academic Publishers, Dordrecht, The Netherlands. 353 pp.

Casagli, N., Rinaldi, M., Gargini, A., Curini, A., 1999. Pore water pressure and streambank stability: results from a monitoring site on the Sieve River, Italy. Earth Surface Processes and Landforms 24, 1095–1114.

Cascini, L., Gullà, G., 1993. Caratterizzazione fisico-meccanica dei terreni prodotti dall'alterazione di rocce gneissiche. Rivista Italiana di Geotecnica 27 (2), 125–147.

Cascini, L., Gullà, G., Sorbino, G., 2006. Groundwater modelling of a weathered gneissic cover. Canadian Geotechnical Journal 43 (11), 1153–1166.

Catani, R., Fabbri, P., Priante, M., Suppo, M., 1995. Caratteri climatici della Calabria. Utilizzazione del coefficiente di variazione per l'individuazione di aree pluviometriche omogenee. Idrotecnica 6, 341–352.

Clerici, A., Perego, S., Tellini, C., Vescovi, P., 2002. A procedure for landslide susceptibility zonation by the conditional analysis method. Geomorphology 48, 349–364.

Clerici, A., Perego, S., Tellini, C., Vescovi, P., 2006. A GIS-based automated procedure for landslide susceptibility mapping by the Conditional Analysis method: the Baganza valley case study (Italian Northern Apennines). Environmental Geology 50 (7), 941–961.

Cruden, D.M., Varnes, D.J., 1996. Landslide Types and Processes. In: Turner, A.K., Schuster, R.L. (Eds.), Landslides: Investigation and Mitigation. Special Report 247, Transportation Research Board, National Research Council. National Academy Press, Washington, D.C., pp. 36–75.

D'Amato Avanzi, G., Giannecchini, R., Puccinelli, A., 2004. The influence of the geological and geomorphological settings on shallow landslides. An example in a temperate climate environment: the June 19, 1996 event in northwestern Tuscany (Italy). Engineering Geology 73, 215–228.

Ercanoglu, M., Gokceoglu, C., 2004. Use of fuzzy relations to produce landslide susceptibility map of a landslide prone area (West Black Sea Region, Turkey). Engineering Geology 75 (3–4), 229–250.

Ermini, L., Catani, F., Casagli, N., 2005. Artificial neural networks applied to landslide susceptibility assessment. Geomorphology 66, 327–343.

ESRI, 2004. ArcGIS 9.0th edition. ESRI, Redlands, CA.

Ghisetti, F., 1979. Relazioni tra strutture e fasi trascorrenti e distensive lungo i sistemi Messina-Fiumefreddo, Tindari-Letojanni e Alia-Malvagna (Sicilia nord-orientale): uno studio microtettonico. Geologica Romana 18, 23–58.

Gomez, H., Kavzoglu, T., 2005. Assessment of shallow landslide susceptibility using artificial neural network in Jabonosa River basin, Venezuela. Engineering Geology 78, 11–27.

Govi, M., Mortara, G., 1981. I dissesti prodotti dal nubifragio del 10 luglio 1972 nella bassa Valle Seriana. Bollettino Associazione Mineraria Subalpina 18 (1–2), 87–118.

Greco, R., Sorriso-Valvo, M., Catalano, E., 2007. Logistic regression analysis in the evaluation of mass movements susceptibility: the Aspromonte case study, Calabria, Italy. Engineering Geology 89, 47–66.

Guinau, M., Pallas, R., Vilaplana, J.M., 2005. A feasible methodology for landslide susceptibility assessment in developing countries: a case-study of NW Nicaragua after Hurricane Mitch. Engineering Geology 80, 316–327.

Gullà, G., Esposito, D., 2003. Caratterizzazione geotecnica di "slurries": risultati preliminari. Tecnical Report, vol. 613. CNR IRPI, Cosenza, Italy. 20 pp.

Gullà, G., Sorbino, G., 1994. Considerazioni sulla permeabilità satura dei materiali di alterazione di origine gneissica. Proceedings of the Symposium Il Ruolo dei Fluidi nei Problemi di Ingegneria Geotecnica. CNR-Gruppo Nazionale di Coordinamento per gli Studi di Ingegneria Geotecnica, 6–7 September 1994, Mondovì, Cuneo, Italy, pp. 85–99.

Gullà, G., Sorbino, G., 1996. Soil suction measurements in a landslide involving weathered gneiss. Proceedings of the VII International Symposium on Landslides, 17–21 June 1996, Trondheim, Norway. A.A. Balkema, Rotterdam, The Netherlands, pp. 749–754.

Gullà, G., Aceto, L., Niceforo, D., 2004a. Geotechnical characterisation of fine-grained soils affected by soil slips. Proceedings of the IX International Symposium on Landslides, 28 June–7 July 2004, Rio de Janeiro, Brasil. A.A. Balkema, Rotterdam, The Netherlands, pp. 663–668.

Gullà, G., Niceforo, D., Ferraina, G., Aceto, L., Antronico, L., 2004b. Monitoring station of soil slips in a representative area of Calabria (Italy). Proceedings of the IX International Symposium on Landslides, 28 June–7 July 2004, Rio de Janeiro, Brasil. A.A. Balkema, Rotterdam, The Netherlands, pp. 591–596.

Gullà, G., Mandaglio, M.C., Moraci, N., Sorriso-Valvo, M., 2004c. Definizione degli elementi generali di modelli geotecnici per l'analisi delle instabilità superficiali per scorrimento-colata in Calabria jonica. Proceedings of the XXII Convegno Nazionale di Geotecnica, 22–24 September 2004, Palermo, Italy. Associazione Geotecnica Italiana, Patron Editore, Bologna, pp. 127–134.

Gullà, G., Mandaglio, M.C., Moraci, N., 2006. Effect of weathering on the compressibility and shear strength of a natural clay. Canadian Geotechnical Journal 43 (6), 618–625.

Guzzetti, F., Reichenbach, P., Ardizzone, F., Cardinali, M., Galli, M., 2006. Estimating the quality of landslide susceptibility models. Geomorphology 81 (1–2), 166–184.

Köppen, W., 1948. Climatologia, con un estudio de los climas de la tierra. Fondo de Cultura Economica, Mexico, Buenos Aires. 479 pp.

Loye-Pilot, M.D., 1984. Coulées boueuses et laves torrentielles en Corse: exemple de mouvements de terrain en pays méditerranéen montagnard.

Mouvements de Terrain, Série Documents du Bureau de Recherche Géologique et Minière, Orléans, France, pp. 23–28.
Monaco, C., Tortorici, L., 2000. Active faulting in the Calabrian Arc and eastern Sicily. Journal of Geodynamics 29, 407–424.
Monaco, C., Tortorici, L., Nicolich, R., Cernobori, L., Costa, M., 1996. From collisional to rifted basins: an example from the southern Calabrian arc (Italy). Tectonophysics 266, 233–249.
Moser, M., Hohensinn, F., 1983/84. Geotechnical aspects of soil slips in Alpine regions. Engineering Geology 19, 185–211.
Ogura, A.T., Filho, O.A., 1991. The Morin Debris-flow Disaster at Petropolis City, Rio de Janeiro State, Brazil. Landslide News 5, 22–24.
Pike, R.J., Howell, D.G., Graymer, R.W., 2003. Landslides and cities — an unwanted partnership. In: Heiken, G., Fakundiny, R., Sutter, J.F. (Eds.), Earth Science in the City — A Reader. American Geophysical Union, Special Publication, vol. 56, pp. 187–254.
Pinna, M., 1977. Climatologia. UTET, Torino, Italy. 442 pp.
Soeters, R., van Westen, C.J., 1996. Slope instability recognition analysis and zonation. In: Turner, A.K., Schuster, R.L. (Eds.), Landslide Investigation and Mitigation. National Research Council, Transportation Research Board Special Report, vol. 247. National Academy Press, Washington, D.C., pp. 129–177.
Sorriso-Valvo, M., 1993. The geomorphology of Calabria. A Sketch. Geografia Fisica e Dinamica Quaternaria 16, 75–80.
Sorriso-Valvo, M., 2002. Landslides: from inventory to risk. In: Rybàř, J., Stemnerk, J., Wagner, P. (Eds.), Landslides, Proceedings of the I European Conference on Landslide, June 24–26 Prague, Cz. Rep. Balkema, Netherland, pp. 79–93.
Sorriso-Valvo, M., Tansi, C., 1996. Grandi frane e deformazioni gravitative profonde di versante della Calabria-Note illustrative per la carta al 250.000. Geografia Fisica e Dinamica Quaternaria 19, 395–408.
Sorriso-Valvo, M., Antronico, L., Gaudio, R., Gullà, G., Iovine, G., Merenda, L., Minervino, I., Nicoletti, P.G., Petrucci, O., Terranova, O., 2004. Carta dei dissesti causati in Calabria meridionale dall'evento meteorologico dell'8–10 settembre 2000. CNR-GNDCI Pubblication, vol. 2859. Rubbettino Publisher, Soveria Mannelli, Italy.
Terranova, O., 2004a. Regional analysis of superficial slope instability risk in Calabria (Italy) through a pluviometrical approach. In: Brebbia, C.A. (Ed.), Risk Analysis IV. WIT Press, Southampton, Boston, pp. 257–266.
Terranova, O., 2004b. Caratteristiche degli eventi pluviometrici a scala giornaliera in Calabria. Proceedings of the XXIX Convegno di Idraulica e Costruzioni Idrauliche, 7–10 September 2004, Trento, Italy. BIOS Publisher, Cosenza, Italy, pp. 343–350.
Terranova, O., Gullà, G., 2004. Hydrological characterisation of possibile triggering scenarios in slope instability. In: Martin-Duque, J.F., Brebbia, C.A., Godfrey, A.E., Diaz de Teran, J.R. (Eds.), Geo-Environment. WIT Press, Southampton, Boston, pp. 123–132.
Terranova, O., Antronico, L., Gullà, G., 2007. Landslide triggering scenarios in homogeneous geological contexts: The area surrounding Acri (Calabria, Italy). Geomorphology 87, 250–267.
Tortorici, L., 1982. Analisi delle deformazioni fragili dei sedimenti postorogeni della Calabria settentrionale. Bollettino Società Geologica Italiana 100, 291–308.
Tortorici, L., Monaco, C., Tansi, C., Cocina, O., 1995. Recent and active tectonics of the Calabrian Arc (Southern Italy). Tectonophysics 243, 37–55.
Tortorici, G., Bianca, M., Monaco, M., Tortorici, L., Tansi, C., De Guidi, G., Catalano, S., 2002. Quaternary normal faulting and marine terracing in the area of Capo Vaticano and S. Eufemia Plain (southern Calabria, Italy). Studi Geologici Camerti 2, 1–16.
Van Asch, Th.W.J., Sukmantalya Kesumajaya, I.N., 1993. The modelling of soil slip erosion in the upper Komering area, South Sumatra Province, Indonesia. Geografia Fisica e Dinamica Quaternaria 16, 81–86.
Versace, P., Ferrari, E., Gabriele, S., Rossi, F., 1989. Valutazione delle piene in Calabria. Geodata, vol. 30. CNR IRPI-GNDCI, Cosenza, Italy. 220 pp.
Westaway, R., 1993. Quaternary uplift of Southern Italy. Journal of Geophysical Research 98, 21741–21772.
Wieczorek, G.F., Larsen, M.C., Eaton, L.S., Morgan, B.A., Blair, J.L., 2001. Debris-flow and flooding hazards associated with the December 1999 storm in coastal Venezuela and strategies for mitigation. U.S. Geological Survey, Open File Report 01-144. 40 pp.